Toward a Neoproterozoic composite carbon-isotope record

Galen P. Halverson[†]
Department of Earth and Planetary Sciences, Harvard University, 20 Oxford Street, Cambridge, Massachusetts 02138-2902, USA and Department of Earth, Atmospheric, and Planetary Sciences, Massachusetts Institute of Technology, Building 54-1126, Cambridge, Massachusetts 02139, USA

Paul F. Hoffman
Daniel P. Schrag
Adam C. Maloof[‡]
Department of Earth and Planetary Sciences, Harvard University, 20 Oxford Street, Cambridge, Massachusetts 02138-2902, USA

A. Hugh N. Rice
Department of Geological Sciences, University of Vienna, Althanstrasse 14, A-1090 Vienna, Austria

ABSTRACT

Glacial deposits of Sturtian and Marinoan age occur in the well-studied Neoproterozoic successions of northern Namibia, South Australia, and northwestern Canada. In all three regions, the Marinoan glaciation is presaged by a large negative δ^{13}C anomaly, and the cap carbonates to both glacial units share a suite of unique sedimentological, stratigraphic, and geochemical features. These global chronostratigraphic markers are the bases of a new correlation scheme for the Neoproterozoic that corroborates radiometric data that indicate that there were three glacial epochs between ca. 750 and 580 Ma. Intraregional correlation of Neoproterozoic successions in the present-day North Atlantic region suggests that glacial diamictite pairs in the Polarisbreen Group in northeastern Svalbard and the Tillite Group in eastern Greenland were deposited during the Marinoan glaciation, whereas the younger of a pair of glacials (Mortensnes Formation) in the Vestertana Group of northern Norway was deposited during the third (Gaskiers) Neoproterozoic glaciation. Gaskiers-aged glacial deposits are neither globally distributed nor overlain by a widespread cap carbonate but are associated with an extremely negative δ^{13}C anomaly. The chronology developed here provides the framework for a new, high-resolution model carbon-isotope record for the Neoproterozoic comprising new δ^{13}C (carbonate) data from Svalbard (Akademikerbreen Group) and Namibia (Otavi Group) and data in the literature from Svalbard, Namibia, and Oman. A new U-Pb zircon age of 760 ± 1 Ma from an ash bed in the Ombombo Subgroup in Namibia provides the oldest direct time-calibration point in the compilation, but the time scale of this preliminary δ^{13}C record remains poorly constrained.

Keywords: Neoproterozoic, chemostratigraphy, carbon isotope, glaciation, geochronology.

INTRODUCTION

Over two decades ago Knoll et al. (1986) documented large and reproducible fluctuations in the carbon-isotope composition of the Neoproterozoic oceans. Noting that these fluctuations track Neoproterozoic ice ages in much the same way that variations in marine δ^{18}O composition define Quaternary glacial cycles, Knoll and Walter (1992) predicted that carbon-isotope chemostratigraphy would prove to be a particularly useful chronostratigraphic correlation tool for late Precambrian rocks. The carbon-isotope database for the Neoproterozoic has proliferated (Shields and Veizer, 2002) over the past decade, and a greatly improved picture of the relationship between δ^{13}C patterns and glaciations is emerging. Nevertheless, the full potential of the carbon-isotope record has not been fully realized, owing in large part to scarce radiometric age constraints from key successions, limited biostratigraphic resolution, and the uncertainty in the number of Neoproterozoic glaciations and δ^{13}C anomalies.

Various workers have compiled composite δ^{13}C records for the Neoproterozoic (e.g., Hayes et al., 1999; Jacobsen and Kaufman, 1999; Walter et al., 2000), but like attempts to construct ^{87}Sr/^{86}Sr records for this time period (Melezhik et al., 2001), these compilations have suffered from low sample density, limited availability of chronostratigraphically well-constrained data, and the consequent dependence on many tenuous correlations. In this paper we present a new, high-resolution δ^{13}C compilation that spans much of the Neoproterozoic and consists of both new and previously published data from Svalbard, Namibia, and Oman. Like the others, this record is based unavoidably on interpretive correlations (Knoll and Walter, 1992) and should be regarded as a preliminary model, but its strength is that it relies on only two linkages: Svalbard-Namibia and Namibia-Oman.

Any chronology for the Neoproterozoic must reconcile the question of the number of glaciations (e.g., Kennedy et al., 1998) that occurred during this era. We concur with various authors who have recently proposed that there were three glacial epochs (Knoll, 2000; Hoffman and Schrag, 2002; Xiao et al., 2004) and use the now conventional names *Sturtian* and *Marinoan* (Dunn et al., 1971) to refer to the older two glaciations. Recently acquired radiometric age constraints (Bowring et al., 2003; Hoffmann et al., 2004) demonstrate unequivocally that the Gaskiers glacials in eastern Newfoundland postdate the Marinoan glaciation (Knoll et al., 2004) (Fig. 1). Although glacial deposits of Gaskiers age appear to be less widespread geographically than their predecessors, intraregional correlations proposed in this study suggest that the upper of a pair of well-studied glaciogenic formations in the Vestertana Group in northern

Norway is also post-Marinoan in age and likely equivalent to the Gaskiers glacials (Fig. 1). Stratigraphic, paleontological, and carbon-isotope data also imply a Gaskiers age for the Hankalchoug diamictite in northwestern China, where Marinoan-aged and putative Sturtian-aged glacial deposits are also present (Xiao et al., 2004).

This paper begins with a review of the Neoproterozoic successions in northern Namibia, northwestern Canada, and South Australia, all of which contain Sturtian- and Marinoan-aged glacial deposits whose correlations are straightforward (Kennedy et al., 1998; Hoffman and Schrag, 2002). Pertinent published stratigraphic, isotopic, and radiometric data from Svalbard, the southwestern United States (Death Valley), Scotland, and Oman are reviewed to broaden the chronology. New carbon-isotope data from Namibia and Svalbard provide detailed pre-Sturtian and post-Marinoan records, while new data from northern Norway support a Gaskiers age for the Mortensnes glacials. This glacial event appears to correspond, at least temporally, to the largest negative $\delta^{13}C$ anomaly in the Proterozoic and is the key to linking the Oman record to the composite $\delta^{13}C$ curve. New Sr isotope data from Namibia and Svalbard and an U-Pb age on an ash bed in the pre-Sturtian Ombombo Subgroup in Namibia reinforce the compilation. Ambiguities in the timing and duration of the glaciations and the scarcity of useful radiometric ages preclude a definitive time-calibration of the $\delta^{13}C$ record at this time. Two permissible but speculative time scales are suggested, but it is expected that the composite $\delta^{13}C$ record will be amended as new data emerge.

ISOTOPIC DATA

Nearly 2000 new carbon-isotope data from Svalbard, Namibia, and Norway are presented in this paper. All carbon-isotope data are presented in per mil (‰) notation using the Vienna Pee Dee Belemnite (VPDB) standard and, along with simultaneously acquired $\delta^{18}O$ data, are available as supplementary online material (Tables DR1–DR5).[1] Analytical methods are described in detail in Halverson et al. (2004).

New $^{87}Sr/^{86}Sr$ data published here (Table DR-6; see footnote 1) are mainly from Sr-rich and Mn-poor samples from Svalbard and Namibia and were measured at the MIT Radiogenic Isotope Laboratory. Following sample purification and carbonate dissolution, Sr was isolated via

standard column chemistry techniques and analyzed on a VG Sector 54 (TIMS) instrument with an average internal precision (2 σ) of 0.000012. See Halverson et al. (2005) for a more detailed discussion of the analytical methods.

U-Pb geochronologic data for zircons from an ash bed in Namibia were acquired by isotope dilution–thermal ionization mass-spectrometry (ID-TIMS) at the same laboratory as above. Analytical procedures are described in detail in Schmitz et al. (2003) and summarized in Table DR-7 (see footnote 1).

Diagenetic Alteration of Isotopic Signals

Diagenetic overprinting of original seawater isotopic signatures is always a concern in ancient carbonates, and it is safe to assume every carbonate sample we have analyzed has experienced some degree of chemical alteration

during recrystallization, dolomitization, and other diagenetic processes. The $\delta^{18}O$ and $^{87}Sr/^{86}Sr$ compositions and trace element concentrations (e.g., Sr and Mn) of carbonates are especially prone to alteration during meteoric diagenesis and dolomitization, and these chemical tracers can be used as one tool to monitor the extent of chemical alteration (Brand and Veizer, 1980, 1981; Banner and Hanson, 1990). Due to the high concentration of C in carbonate rocks, relative to meteoric fluids, the $\delta^{13}C$ composition of carbonate rocks is much more resistant to chemical overprinting than $\delta^{18}O$, for example. Many previous studies have addressed the fidelity of $\delta^{13}C$ signatures in Neoproterozoic carbonates and the typical conclusion is that even clearly diagentically altered and dolomitized carbonates appear to preserve their original $\delta^{13}C$ composition (e.g., Kaufman et al., 1991; Derry et al., 1992; Kaufman and Knoll, 1995;
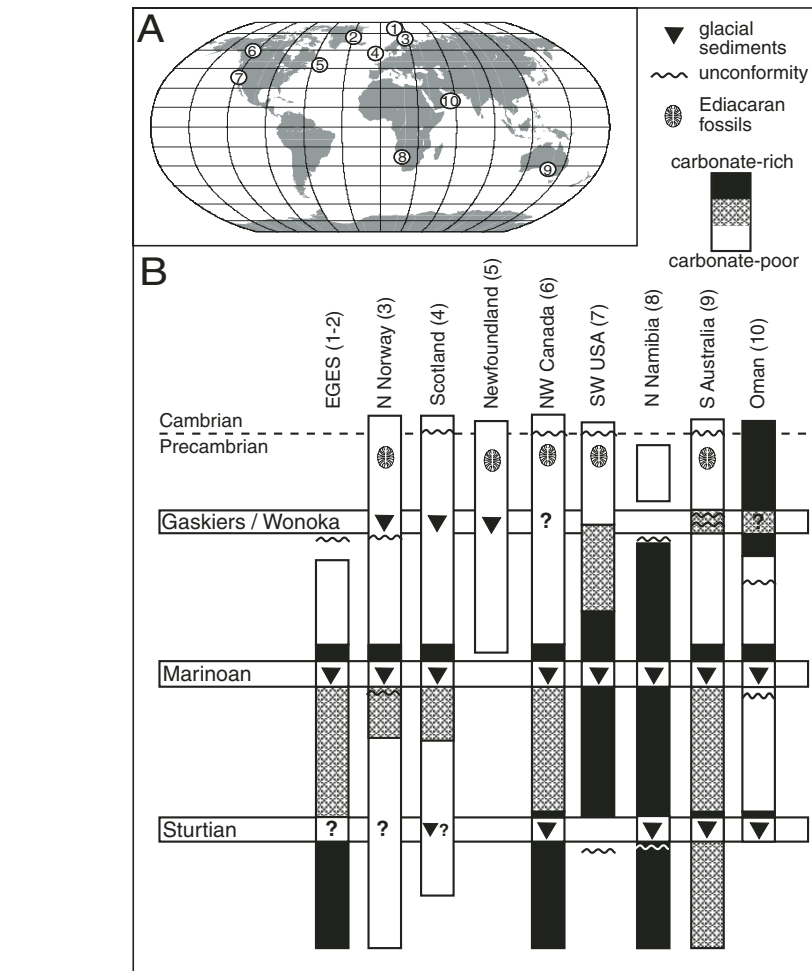

Figure 1. (A) Present-day locations of the Neoproterozoic successions discussed in this paper. (B) Schematic profiles of the successions from (A), showing their stratigraphic range, simplified lithologies, distribution of glacial deposits, and occurrence of Ediacaran fossils. See text for references. EGES—East Greenland-East Svalbard platform.

Brasier et al., 1996). Our own detailed studies on Namibian and Svalbard carbonates (Halverson et al., 2002, 2004, 2005) have demonstrated that even below major exposure surfaces and in rocks in contact with paleoaquifers, $\delta^{13}C$ signatures are resistant to overprinting and major trends are reproducible basinwide.

The process that can alter carbonate $\delta^{13}C$ compositions most severely is the incorporation of ^{13}C-depleted carbon from the oxidation of organic matter or methane during diagenesis (e.g., Irwin et al., 1977). We have found isolated evidence for such alteration of carbonates in Svalbard (Halverson, 2003; Halverson et al., 2004) and do not include these samples in this contribution. Cases of extreme spatial variability in $\delta^{13}C$ signatures due to incorporation of methane-derived C have been documented in Neoproterozoic cap carbonates in southern China (Jiang et al., 2003a; Bao et al., 2004) and are a reminder that this process can drastically affect isotopic signatures locally. Although it is difficult to ascertain more subtle effects from incorporation of organic-derived C, we note that most of the samples we have analyzed from Namibia, Svalbard, and Norway have low organic matter contents and should therefore be relatively immune to this type of isotopic alteration.

Whereas we believe that the $\delta^{13}C$ data presented here broadly record original depositional signatures, since we have not subjected each sample to systematic diagenetic screening, nor can we exclude the possibility of minor diagenetic effects, we stress that the data presented in this paper are not considered exact proxies for seawater $\delta^{13}C$. We assume a standard error of $\pm 1‰$ on all our carbon-isotope data (Halverson et al., 2002), which is small compared to the amplitude of variability of $\delta^{13}C$ in marine carbonates and comparable in magnitude to intrabasinal variability, as discussed later.

REFERENCE SECTIONS

Over thirty years ago, Dunn et al. (1971) correlated the Sturtian and Marinoan glacial deposits and their associated cap carbonates across Australia and postulated that they could be used as global chronostratigraphic markers. Although correlations have not proven to be straightforward everywhere, this hypothesis has essentially been borne out (Kennedy et al., 1998; Walter et al., 2000; Hoffman and Schrag, 2002). The Sturtian and Marinoan glacials in Australia (Preiss, 2000) correlate unambiguously with glacial pairs in the classic Neoproterozoic successions of northern Namibia (Hoffmann and Prave, 1996) and the northern Canadian Cordillera (Aitken, 1991b; Narbonne and Aitken, 1995). These three successions

(Fig. 2) share several key features, including distinct Sturtian and Marinoan cap carbonate sequences (Hoffman and Schrag, 2002) and a characteristic sub-Marinoan negative $\delta^{13}C$ anomaly (*Trezona* anomaly). In each succession, banded iron formation (BIF) is localized within the Sturtian glacials. Collectively, these successions constitute the foundation of the Neoproterozoic correlation scheme.

Given the contrast in overall lithology between the three successions—dominantly carbonate in Namibia, dominantly terrigenous in Australia, and mixed terrigenous and carbonate in Canada—the uniformity of the respective cap carbonates and isotope anomalies is striking (Kennedy et al., 1998; Hoffman and Schrag, 2002). This gives us confidence that the glacials can be correctly identified in regions where only one is present or where one glacial masquerades as two. We first summarize existing knowledge of the three founding successions, highlighting aspects of their stratigraphy, sedimentology, and isotopic chemistry that aid correlation with other successions.

Northern Namibia

The Otavi Group (Fig. 3) is exposed in a Pan-African fold belt rimming the southwestern promontory of the Congo craton in Namibia. It is conformably underlain by fluviatile clastics of the Nosib Group and disconformably overlain by marine and fluviatile clastics of the Mulden Group. The latter are interpreted as foreland basin deposits associated with collision between the Congo craton and the frontal magmatic arc of southeastern coastal Brazil (Stanistreet et al., 1991; Cordani et al., 2003). The best estimate for the age of this collision and for the end of Otavi carbonate deposition is ca. 580 Ma, the onset of widespread contractional deformation on the distal western margin of the Congo craton in Namibia (Goscombe et al., 2003). During Otavi Group time, the shallow-water Otavi carbonate platform in the north was progressively differentiated from the deep-water Outjo basin to the south (Fig. 3). The facies transition (Fransfontein foreslope) between the two is well defined. The differentiation was initiated by north-south crustal stretching, which began in the lower Otavi Group and is dated by U-Pb ages (Fig. 3) on volcanic rocks in the Ombombo Subgroup ranging from 760 ± 1 Ma to 746 ± 2 Ma (Hoffman et al., 1996). These ages predate the syn-rift, glaciogenic Chuos Formation, which represents the Sturtian glaciation and defines the base of the Abenab Subgroup (Fig. 3).

Crustal stretching continued until middle Abenab time (Halverson et al., 2002), but the younger glacial marine diamictite complex,

the Ghaub Formation, is stratigraphically conformable regionally, and was deposited on a thermally subsiding passive margin (Halverson et al., 2002). Therefore, Ghaub glaciation on the Otavi platform was not associated with rifting, as is often proposed (Eyles, 1993; Young, 1995; Eyles and Januszczak, 2004). A Marinoan age for the Ghaub Formation (Kennedy et al., 1998) has been confirmed by a new U-Pb zircon age of 635.5 ± 1.2 Ma on an intraglacial tuff bed in central Namibia (Hoffmann et al., 2004). The postrift thickness of the carbonate platform, mostly comprising the Tsumeb Subgroup, is 1.6 km in the west (Fig. 3) and nearly 3.5 km in the east (Fig. 3; King, 1994).

The Chuos Formation (Hoffmann and Prave, 1996) is dominated by heterolithic, matrix-rich, subglacial and proximal rain-out diamictite. The diamictite matrix is ferruginous throughout, and thin units of iron formation occur here and there. The bulk thickness of the Chuos glacials is highly variable —absent on paleotopographic highs and up to 1000 m thick in corresponding lows (Fig. 3). The basal Chuos deposits bevel the underlying Ombombo Group strata at a low angle (1.5°), meaning that there is a substantial and variable hiatus between the top of the Ombombo Subgroup and the basal Chuos diamictite, which attests to the active extensional regime in which the glaciation occurred. We believe the resulting topography is largely responsible for the greater overall volume of Chuos diamictite, compared to the Ghaub, and for the fact that the Chuos is much richer in extrabasinal debris.

The Chuos Formation ends abruptly at a major flooding surface overlain by the Rasthof Formation, a quintessential Sturtian cap-carbonate sequence. On the Otavi platform, it stands out as a single shoaling-upward (highstand) 200–400-m-thick depositional sequence, contrasting with stacks of much thinner parasequences comprising the nonglacial strata above and below. In platformal sections, the basal Rasthof member is a dark, fetid, ^{13}C-depleted, limestone rhythmite with thin dolomitic turbidites (Yoshioka et al., 2003). The abiotic rhythmites are abruptly overlain by >100 m of strictly subaqueous, dolomite microbialaminite. There is a sharp shift to positive $\delta^{13}C$ values at the contact but no break in sedimentation. The microbialaminite is wildly contorted and contains characteristic "roll-up" structures, showing that the microbial-bound laminae were cohesive but pliable when ripped up. The microbialaminite is remarkably continuous vertically, with no sign of subaerial exposure. It passes imperceptibly near the top of the formation into dolomite grainstone that coarsens upward to a major subaerial exposure surface. The Rasthof Formation is more
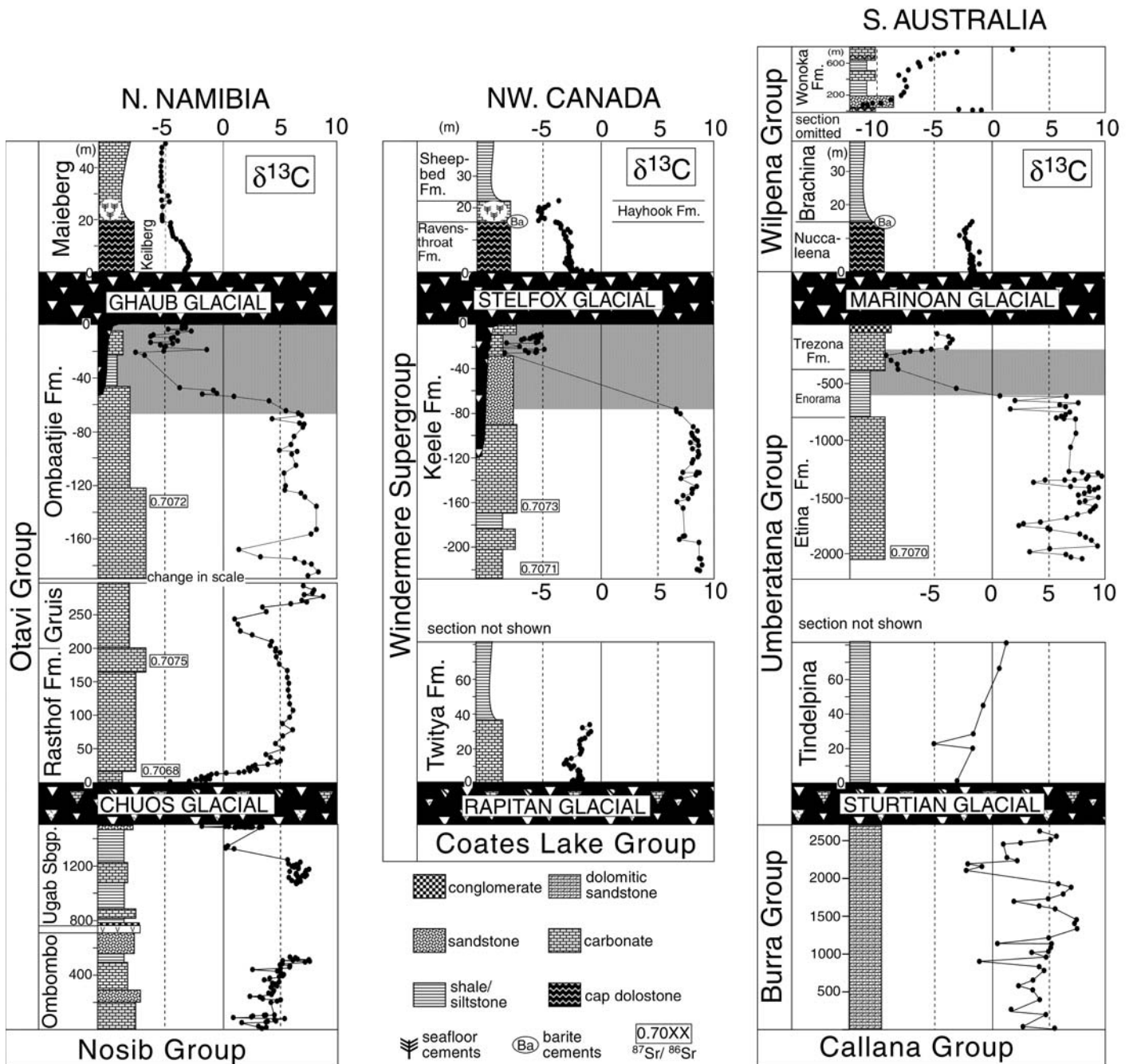
Figure 2. Composite carbon-isotope profiles and simplified stratigraphic columns spanning the inferred Sturtian and Marinoan glaciations in northern Namibia (δ^{13}C data from Hoffman and Schrag, 2002; Halverson et al., 2002; this paper. ^{87}Sr/^{86}Sr data from Yoshioka et al., 2003; this paper), northwestern Canada (δ^{13}C data from Hoffman and Schrag, 2002; James et al., 2001. ^{87}Sr/^{86}Sr data from Narbonne et al., 1994; Kaufman et al., 1997), and South Australia (δ^{13}C data from Hoffman and Schrag, 2002; McKirdy et al., 2001; Hill and Walter, 2000. ^{87}Sr/^{86}Sr data from McKirdy et al., 2001). Shaded background delineates the pre-Marinoan (*Trezona*) negative δ^{13}C anomaly, first documented in detail in South Australia by McKirdy et al. (2001). Note the absence of a similar anomaly in the pre-Sturtian record of Namibia and Australia. This figure is modified from Halverson et al. (2004) and Hoffman and Schrag (2002). Note variable thickness scales.
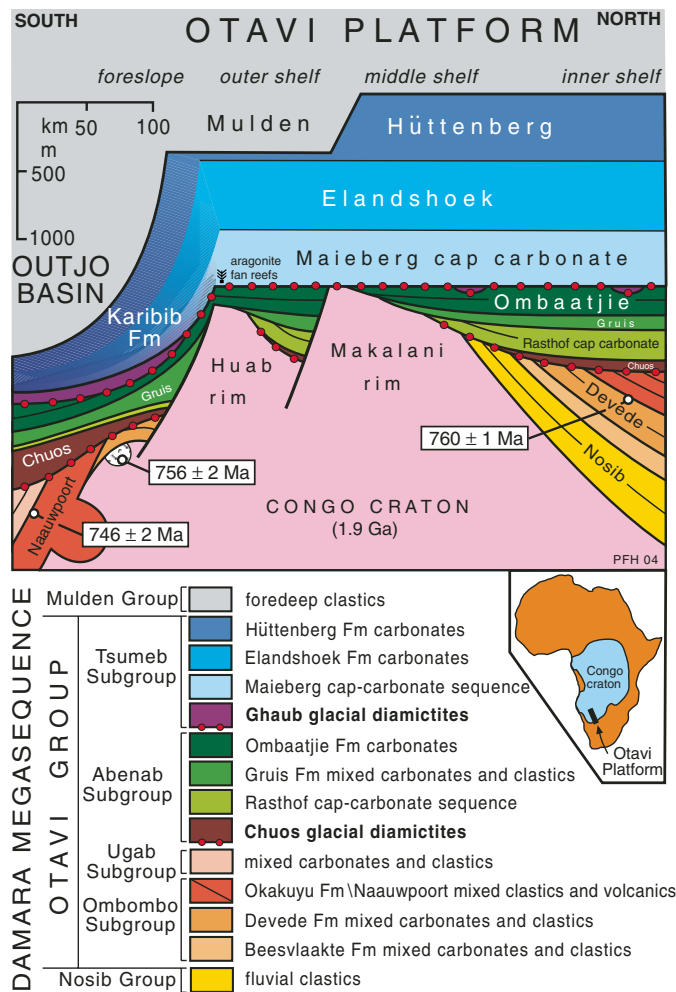
Figure 3. Schematic stratigraphic cross section across the Otavi platform and Outjo basin on the southern margin of the Congo craton (see inset) in northern Namibia, modified from Halverson et al. (2002). U-Pb zircon age constraints (white boxes and circles) are from Hoffman et al., 1996 (746 ± 2 and 756 ± 2 Ma) and this paper (760 ± 1 Ma). See Hoffmann and Prave (1996) for details of stratigraphic nomenclature, except for formation names in Ombombo Subgroup, which are introduced informally here.

The 300–400-m-thick Maieberg Formation is the cap carbonate sequence overlying the Ghaub glacial surface on the Otavi platform (Hoffman and Schrag, 2002). The basal Keilberg Member (Hoffmann and Prave, 1996) is an ~20-m-thick transgressive cap dolostone, which presents a characteristic suite of sedimentary structures, including microbial bioherms with tubular and sheeted infillings (Hoffman et al., 2002) and steep wave-generated megaripples (Allen and Hoffman, 2005). The top of the Keilberg Member is a major flooding surface, overlain by marly rhythmites and a thick succession of pink limestone with gravity flow deposits and large-scale swaley crossbeds. Locally on the Huab rim and elsewhere on the platform, buildups of originally aragonite, sea-floor cements occur directly above the flooding surface (Hoffman and Schrag, 2002). In many regions (e.g., Australia, Canadian Cordillera, Svalbard, Oman), the aftermath of the Marinoan glaciation is dominated by terrigenous sediment. In others (e.g., western Africa, southern China), the post-Marinoan section is strongly condensed. Therefore, the 1.4–3.2 km of carbonates in the Tsumeb Subgroup (Fig. 3) provide a rare opportunity to track geochemical variations in the post-Marinoan ocean.

Northern Canadian Cordillera

The Windermere Supergroup is continuously exposed for >600 km in the Mackenzie Mountains foreland thrust-and-fold belt of the northern Canadian Cordillera (Fig. 1). It comprises <10 km of rift and succeeding shelf-slope sediments of post–780 Ma, pre–Early Cambrian age (Narbonne and Aitken, 1995). To the northeast the Windermere Supergroup is cut out between the Early Cambrian transgression and underlying, pre–780 Ma (Jefferson and Parrish, 1989; Harlan et al., 2003) carbonates of the Little Dal Group (Aitken, 1989). The Windermere Supergroup was initiated by crustal stretching and deposition of the Coates Lake Group, a mixed assemblage of clastics, restricted carbonates, and evaporites that unconformably overlies the Neoproterozoic Little Dal Group (Aitken, 1982). The succeeding Rapitan Group is a nonvolcanic, rift-basin assemblage contemporaneous with the Sturtian glaciation (Eisbacher, 1978; Yeo, 1981). The Marinoan glaciation is represented by carbonate-clast diamictites (Stelfox Member) of the Ice Brook Formation (Aitken, 1991a), situated 700–1400 m above the Rapitan Group in the middle part of the Windermere succession.

The Rapitan Group postdates a widespread 780 Ma mafic igneous event in the Cordillera (Harlan et al., 2003), and a marginally better

spatially variable along the southern margin of the evolving platform (Fig. 3), where the basal ^{13}C-depleted member is commonly missing.

On the platform, the Ombaatjie Formation (Fig. 3) comprises an aggradational stack of 6–8 transgressive-highstand parasequences, each bounded by semicontinuous exposure surfaces. After reaching a high of >8‰, δ^{13}C values plummet by >10‰ in an unremarkable 25–45 interval in the upper part of the formation (Halverson et al., 2002). We refer to this global isotopic event as the *Trezona* anomaly, after the formation in South Australia where it was first well documented (McKirdy et al., 2001). In the most complete sections, δ^{13}C values rise noisily to –4‰ to –3‰ following the smooth decline (Fig. 2). Using a simple thermal subsidence model, the steep

decline in δ^{13}C is estimated to have spanned at least 0.5×10^6 years and to have preceded the sea-level fall presaging the Ghaub glaciation by >1.0 $\times 10^6$ years (Halverson et al., 2002).

The Ghaub Formation is composed predominantly of matrix-rich, carbonate-clast (dolomite and limestone) diamictite, almost exclusively derived from the underlying Abenab Subgroup. It is patchy and very thin (<3 m) on the Otavi platform in most areas, but >1000 m of mixed carbonate-basement clast diamictite locally occurs near the eastern end of the Otavi fold belt (Hedberg, 1979). The formation is continuous and 40–80 m thick on the lower Fransfontein foreslope where it is interpreted to record a single ice advance-and-retreat cycle (Domack and Hoffman, 2003).

maximum age constraint is provided by a 755 ± 18 Ma granite clast in the lower Rapitan Group (Ross and Villeneuve, 1997). Its three formations lithologically resemble the Marinoan glacial sequence in Svalbard and eastern Greenland (Halverson et al., 2004). The basal Mount Berg Formation (Yeo, 1981) is a locally developed, glaciogenic diamictite composed of intrabasinal debris. It is overlain by the more extensive Sayunei Formation, consisting of <700 m of maroon siltstone with fine-grained ferruginous turbidites, carbonate-clast debris flows, and lonestones (Eisbacher, 1978; Yeo, 1981). Banded iron formation, locally bearing large granitoid lonestones, occurs here and there at the top of the Sayunei Formation or within the basal diamictites of the overlying Shezal Formation (Yeo, 1981). The Shezal is typically 300–800 m thick and consists of maroon or olive-colored, heterolithic diamictite and sandstone. The Shezal diamictites truncated the Sayunai Formation, but a dominantly submarine origin is inferred from the absence of ice-contact deposits. Paleomagnetic poles for the Sayunei Formation and the broadly contemporaneous (723 Ma) Franklin igneous suite indicate that the Rapitan Group originated very close to the paleo-Equator (Park, 1997).

The Shezal Formation is capped by 0–40 m of dark, fetid, ^{13}C-depleted, turbiditic limestone (Narbonne et al., 1994), strongly reminiscent of the basal member of the Sturtian Rasthof cap carbonate in Namibia. It forms the base of the Twitya Formation, a 300–800-m-thick transgressive-highstand sequence composed of dark gray siltstones and fine-grained sandstones (Narbonne and Aitken, 1995). The overlying Keele Formation (200–600 m) is a stack of shallow-water marine parasequences dominated variably by cross-bedded sandstone and dolomitized grainstone (Day et al., 2004). δ^{13}C hovers near 8‰ (Narbonne et al., 1994; Hoffman and Schrag, 2002) in the middle of the Keele Formation (the "Keele Peak" of Kaufman et al., 1997) but is strongly ^{13}C-depleted in intraclastic limestones that comprise the youngest member of the formation (Fig. 2). The isotopically negative carbonates beneath the Ice Brook Formation presumably record the tail end of the Trezona anomaly, although underlying clastics mask the decline from strongly enriched isotopic values (Fig. 2) in the main part of the Keele platform (James et al., 2001).

The Ice Brook Formation (Aitken, 1991a, 1991b) comprises slope-facies equivalents of the Keele Formation plus the overlying Marinoan glaciomarine diamictites, which pinch out landward of the Keele shelf break. The basal Durkan Member is a megabreccia related to submarine mass failure of the Keele carbon-

ate platform (Aitken, 1991a). It is overlain by nonglacial siltstones of the Delthore Member. Finally, the 0–300-m-thick (typically 30 m; Aitken, 1991a, 1991b) Stelfox Member is a matrix-rich, carbonate-clast diamictite, with associated ice-rafted horizons of glaciomarine origin.

The transgressive portion of the Marinoan cap carbonate sequence is exceptionally well preserved in the Mackenzie Mountains (Aitken, 1991a; James et al., 2001; Hoffman and Schrag, 2002). It consists of two units (James et al., 2001): the Ravensthroat Formation, a pale-colored dolomite that is regionally continuous (3–20 m thick) atop the Stelfox diamictite and its equivalent disconformity, and the overlying Hayhook Formation, a dark gray and red limestone characterized by formerly aragonite sea-floor cements, which is discontinuously developed (0–14 m thick) near the shelf break in the central and southern Mackenzie Mountains. The cap dolostone (Ravensthroat) consists of laminations of reverse-graded, loosely packed macropeloids, thinly draped by micropeloids. Low-angle cross-lamination is ubiquitous. Locally, meter- to decameter-sized microbial bioherms developed and contain vertical sheetlike infillings of micropeloids. Tubelike structures, which are common in the equivalent bioherms of California (Cloud et al., 1974), Namibia (Hegenberger, 1987), and southwestern Brazil (Nogueira et al., 2003), are not found in the Mackenzie Mountains. The upper half of the cap dolostone is dominated by strongly aggradational, wave-generated megaripples ("tepees" of Aitken, 1991a; James et al., 2001) of unusual size and steepness (Hoffman and Schrag, 2002), which are interpreted to have formed at depths >200 m during a period of intense, sustained winds (Allen and Hoffman, 2005). Similar megaripples occur at the same stratigraphic horizon in Namibia (Hoffman et al., 2002), Brazil (Nogueira et al., 2003), Svalbard (Halverson et al., 2004), and central Australia (Kennedy, 1996).

In the Mackenzie Mountains, the final 10 cm of cap dolostone contains macroscopic seafloor cements composed of primary barite (Hoffman and Schrag, 2002). The cement-rich layer is regionally extensive, but the barite has been dissolved in most areas leaving behind calcite pseudomorphs or a small-scale breccia horizon. Barite cements occur at the identical horizon in the Marinoan cap dolostones of central Australia (Kennedy, 1996). The top of the barite cement layer marks the end of peloidal dolomite production (although some reworking continues) and the onset of lime micrite sedimentation and sea-floor aragonite crystal-fan development, with no significant break in aggradation.

South Australia

The Adelaide Succession of South Australia was deposited in a rapidly subsiding basin and preserves a thick and well-studied record (Preiss, 2000 and references therein). The Sturtian and Marinoan glacial units make up the top and bottom of the Umberatana Group. The Sturtian glacials are constrained to be younger than 777 ± 7 Ma from a U-Pb age on the Boucaut Volcanics at the base of the underlying Burra Group (Preiss, 2000). A U-Pb age of 657 ± 17 Ma (Ireland et al., 1998) on detrital zircons in the Marino Arkose Member in the Enorama Shale (Umberatana Group) provides the only published U-Pb age constraint for the onset of the Trezona anomaly (Fig. 2). No radiometric ages are available for the thick stack of clastic sediments in the overlying Wilpena Group, which includes the Acraman ejecta horizon (Gostin et al., 1986), the Wonoka paleovalleys (von der Borch et al., 1982), and the type locality of Ediacaran fossils (Jenkins et al., 1983).

The Sturtian glacial deposits (Yudnamutana Subgroup; Preiss et al., 1998) overlie a widespread erosional unconformity and range from 0 to 6000 m in thickness (Dunn et al., 1971; Preiss et al., 1998). Like Namibia and Canada, the Sturtian glacials are highly heterolithic and locally contain abundant iron formation (Preiss, 2000). The iron formation is concentrated near the transition with the Benda Siltstone (Braemar ironstone facies; Lottermoser and Ashley, 2000), which separates the Sturtian diamictites from the Tapley Hill cap carbonate sequence. The ~1.5-km-thick Tapley Hill Formation is stratigraphically similar to both the Rasthof and Twitya cap carbonates sequences, with a basal maximum flooding surface that is overlain by interbedded black shales and isotopically negative dolomicrites (Tindelpina Shale) that grade upward into coarser-grained sediments (McKirdy et al., 2001).

The middle Umberatana Group preserves the highly ^{13}C-enriched carbonates of the Keele Peak and is typical of other interglacial successions (Fig. 2; McKirdy et al., 2001). The Trezona δ^{13}C anomaly begins in the lower Enorama Formation and spans many hundreds of meters of section, testament to the rapid subsidence of the basin. Similar to the case in Canada, the negative δ^{13}C shift is partly concealed by an interval of clastic sediments, but highly negative values are recorded in shallow-water carbonates of the Trezona Formation (Fig. 2; McKirdy et al., 2001). A return to more positive δ^{13}C values beneath the Marinoan glacial deposits (Fig. 2; McKirdy et al., 2001) mirrors similar trends seen in many other successions, including Namibia (Halverson et al., 2002).

Shales and sandstone of the Yaltipena Formation separate the Trezona Formation from the overlying Marinoan (Elatina Formation) glacial deposits (Preiss, 2000). The Elatina Formation consists mostly of glacial outwash sandstone with lenses of diamictite, and, in deeper water settings, dropstone-bearing siltstone (Preiss, 2000). The Nuccaleena cap dolostone forms the base of the Brachina cap carbonate sequence (Hoffman and Schrag, 2002), and along with equivalent cap dolostones in Australia, is generally thin (2–10 m), similar isotopically (Fig. 2) to the Keilberg and Ravensthroat cap dolostones, and consists of thin-bedded, microcrystalline dolomite with graded peloid beds and fibrous marine cements (Williams, 1979; Kennedy, 1996). Small barite crystal clusters occur at the top of the cap dolostone in some sections in the Amadeus and Ngalia basins (Kennedy, 1996) and everywhere the dolostone passes upward into purplish siltstones of the Brachina Formation and equivalent units. The Brachina siltstones were deposited during the same highstand as the lower Sheepbed Formation black shales in Canada and the Maieberg Formation pink limestones in Namibia.

A large post-Marinoan negative $\delta^{13}C$ anomaly occurs in South Australia, well above the Brachina Formation (Fig. 2). The *Wonoka* anomaly spans the Wonoka Formation, which contains a well-known, kilometer-deep paleovalley (von der Borch et al., 1982; Christie-Blick et al., 1990). $\delta^{13}C$ drops to a low of <–10‰ beneath an incision surface in the lower Wonoka Formation, and intermittent carbonates remain highly ^{13}C-depleted for over 400 m (Fig. 2; Pell et al., 1993; Calver, 2000). This anomaly is not preserved (at least in full) in either northern Namibia or northwestern Canada, but, as will be discussed below, is found in several other sections, suggesting that it records a global perturbation to the carbon cycle.

OTHER SUCCESSIONS

Svalbard

The Neoproterozoic middle–upper Hecla Hoek Succession comprises the Veteranen, Akademikerbreen, and Polarisbreen groups and outcrops in a north-trending fold-and-thrust belt in northeastern Svalbard (Fig. 4). Now part of the Barents Shelf, eastern Svalbard is widely considered once to have been part of Laurentia and contiguous with eastern Greenland (Knoll et al., 1986; Fairchild and Hambrey, 1984) as part of what is hereafter referred to as the EGES (East Greenland–East Svalbard) platform (Halverson et al., 2004). Paleomagnetic data from Laurentia (Park, 1997; Evans, 2000) suggest

that this basin sat in the tropics throughout much of the middle Neoproterozoic. The base of the ~4-km-thick Veteranen Group siliciclastics is constrained to be younger than ca. 940 Ma from U-Pb zircon ages on basement granites (Gee et al., 1995; Johansson et al., 2000). The minimum age of the Polarisbreen Group is also poorly constrained, and no Ediacaran fossils are present beneath the overlying Cambrian Tokammane Formation (Knoll and Swett, 1987).

The ~1-km-thick mixed clastic–carbonate Polarisbreen Group contains two distinct diamictites (Fairchild and Hambrey, 1984, 1995; Harland et al., 1993): the older Petrovbreen Member (middle Elbobreen Formation) and the younger Wilsonbreen Formation. The Russøya Member comprises the sediments between the Akademikerbreen and the base of the Petrovbreen glacials (Figs. 4 and 5). It includes a basal, upward-shoaling sequence (90–160 m) of black shale with fine dolomite intercalations, molar tooth limestone, and sublittoral microbialites, overlain by a series of thinner parasequences (Fairchild and Hambrey, 1984; Halverson et al., 2004). $\delta^{13}C$ rises through the lower Russøya to a high of 7‰, before falling to –5‰ in the upper Russøya (Halverson et al., 2004) beneath a karstic disconformity below the Petrovbreen Member diamictite (Fig. 5).

The thin Petrovbreen Member diamictite consists of debris plucked from the underlying platform and glacially redeposited in a marine setting (Hambrey, 1983; Fairchild and Hambrey, 1984; Harland et al., 1993). The Petrovbreen Member diamictite is not succeeded by a cap carbonate sequence, but rather by a thick stack of rhythmites comprising the overlying MacDonaldryggen Member (Halverson et al., 2004). These otherwise featureless rhythmites contain calcite pseudomorphs interpreted by Halverson et al. (2004) as glendonites. As glendonites are paleoindicators of sedimentation in cold waters (Kemper and Schmitz, 1981; Swainson and Hammond, 2001), this interpretation implies that cold conditions persisted long after deposition of the Petrovbreen diamictite and is consistent with the absence of an abrupt facies change above the Petrovbreen diamictite, as would be expected if this contact represented the abrupt end of glaciation.

An ~20-m-thick dolomite grainstone (Slangen Member) separates the rhythmites from the glaciogenic Wilsonbreen Formation above, and although brecciated at its top (Fairchild and Hambrey, 1984), shows no sign of erosional truncation (Halverson et al., 2004). The Wilsonbreen Formation is much thicker (~100 m) and more heterogeneous than the Petrovbreen diamictite, consisting of ice-contact tills with

intrabasinal and exotic clasts, cross-bedded sandstone, shales, and rare stromatolites, all deposited in a continental setting (Hambrey, 1982; Fairchild and Hambrey, 1984; Harland et al., 1993). The Dracoisen cap dolostone sharply overlies the Wilsonbreen Formation (Fairchild and Hambrey, 1984; Harland et al., 1993) and forms the transgressive base of the Dracoisen cap carbonate sequence. The 3–15-m-thick, yellow to buff-weathering cap dolostone contains megaripples and peloids and has a highly reproducible $\delta^{13}C$ composition of –3‰ to –4‰ (Fig. 5; Halverson et al., 2004). The cap dolostone grades upward into red siltstone, which then passes into green then black shales deposited during a depositional highstand (Halverson et al., 2004). With the exception of seafloor cements, this cap carbonate sequence is nearly identical to the Ravensthroat-Hayhook-Sheepbed cap carbonate sequence in northwestern Canada (Halverson et al., 2004). Thus, whereas the two Polarisbreen diamictites have been regarded as belonging to two distinct glacial episodes (e.g., Knoll et al., 1986; Fairchild and Hambrey, 1995; Kaufman et al., 1997; Kennedy et al., 1998), new isotopic and stratigraphic evidence (Halverson et al., 2004) suggests instead that these diamictites record the initial and final stages of the global Marinoan glaciation on the EGES platform (Fig. 5).

Accepting the two Polarisbreen diamictites as Marinoan, it follows that the Sturtian glaciation should be represented somewhere in the underlying stratigraphy (Knoll, 2000). However, no glacial deposits have been identified that would positively identify the Sturtian glaciation, and given the limited area of outcrop and lack of contrasting depositional environments (i.e., no foreslope deposits), none are likely to be found. Nonetheless, barring depositional hiatus or erosional removal, the Sturtian cap carbonate should be preserved as a proxy of the glaciation (Knoll, 2000). A pronounced interval of negative $\delta^{13}C$ values, bracketed by sequence boundaries, does occur in the middle Akademikerbreen Group but for reasons discussed below is regarded here as entirely pre-Sturtian. The most likely candidate for a Sturtian cap carbonate sequence then falls at the base of the Polarisbreen Group, where a prominent rise in $\delta^{13}C$ occurs within the lower Russøya Member. The abrupt influx of siliciclastic sediments and onset of high-order cyclicity in the uppermost Akademikerbreen Group may be indirect manifestations of glaciation.

Death Valley

The Neoproterozoic succession in the Death Valley region of the southwestern United States
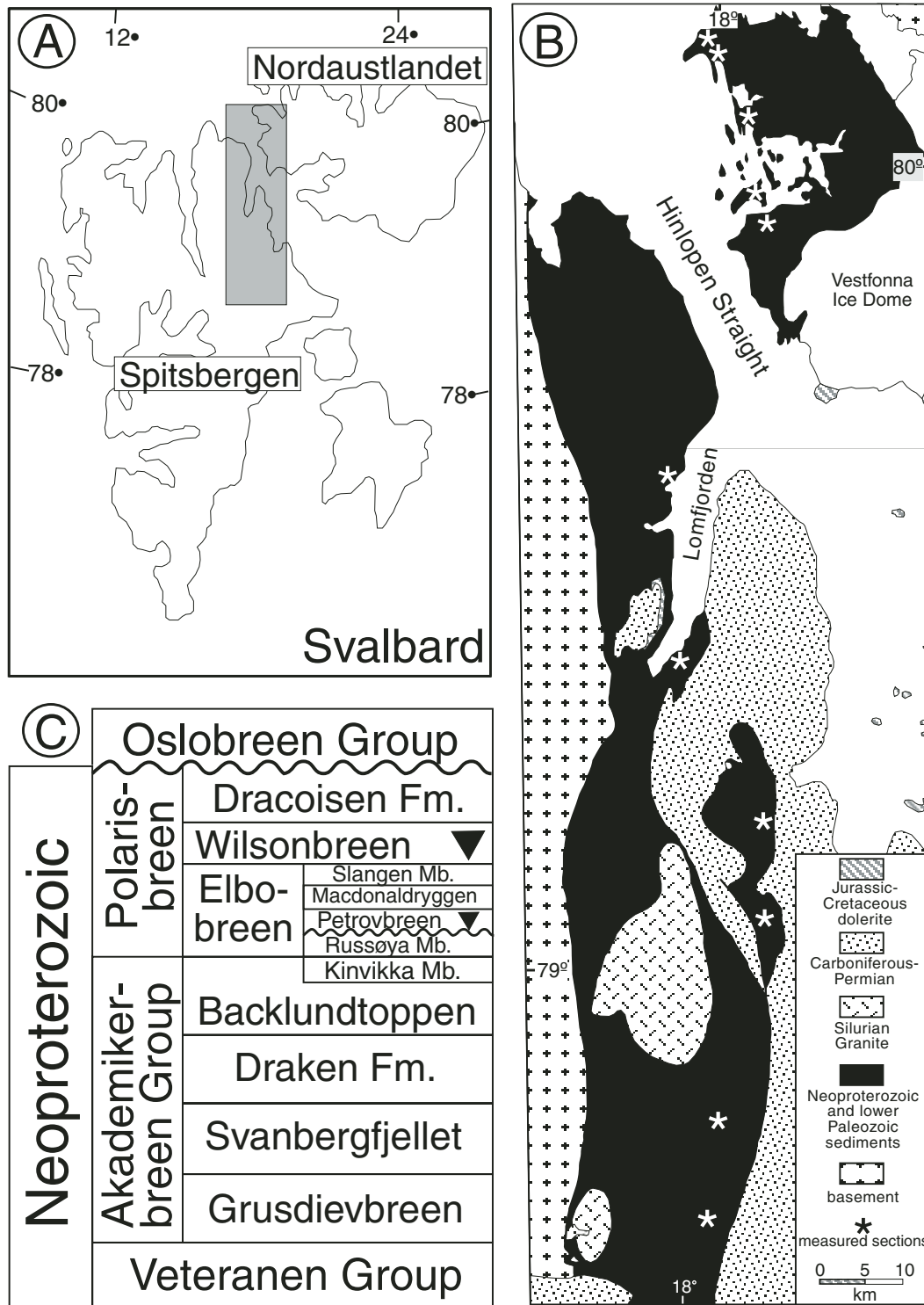
Figure 4. (A) Location map for the Svalbard archipelago on the Barents Shelf. Shaded inset box shows location of the (B) outcrop belt of the Neoproterozoic middle–upper Hecla Hoek Succession (modified from Harland et al., 1992) and locations of stratigraphic sections measured in this study. (C) Stratigraphic nomenclature of the Neoproterozoic succession in northeastern Svalbard. Shaded triangles indicate glacial units.
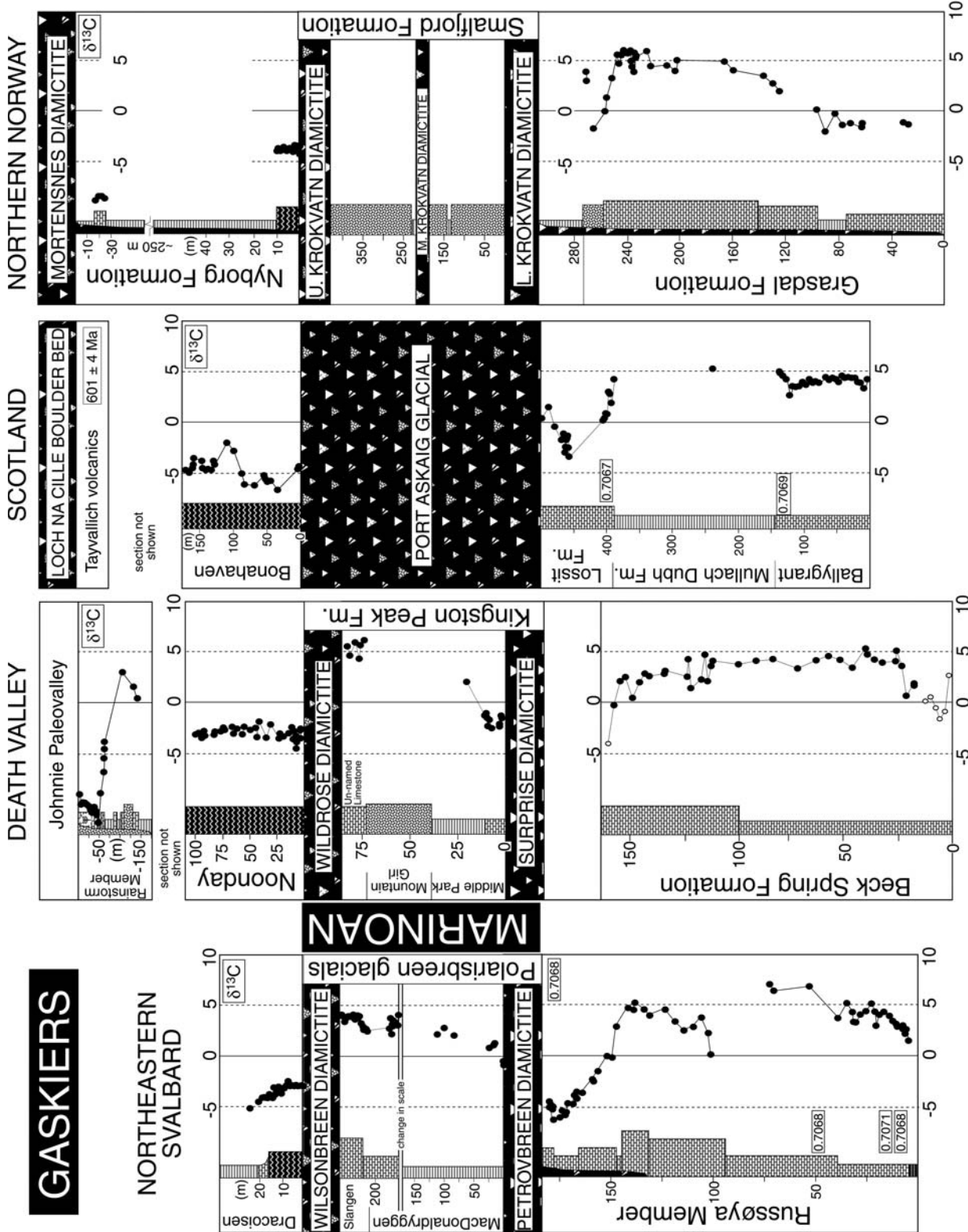
Figure 5. Composite stratigraphic and carbon-isotope profiles spanning the Marinoan and Varanger glaciations and illustrating intraregional correlations of four successions where, based on the correlations in this paper, glacial deposits of Sturtian age are either absent or ambiguous: upper Hecla Hoek Succession in northeastern Svalbard (δ13C data and stratigraphy from Halverson et al., 2004. 87Sr/86Sr data from this paper), the Pahrump Group in Death Valley (δ13C data and stratigraphy from Corsetti and Kaufman, 2003; Prave, 1999a), the Dalradian Supergroup in Scotland (δ13C and 87Sr/86Sr data and stratigraphy from Brasier and Shields, 2000. U-Pb zircon age on the Tayvallich volcanics from Dempster et al., 2002), and the Vestertana Group and Grasdal Formation in northern Norway (δ13C data in Table DR-1 (see footnote 1); stratigraphy from this paper and Siedlecka and Siedlecki, 1971; Edwards, 1984; Føyn and Siedlecki, 1980). Note variable thickness scales. See Figure 2 for legend.

has been the focus of several recent papers bearing on the number of Neoproterozoic glaciations (e.g., Prave, 1999a; Corsetti and Kaufman, 2003). Central to this debate is the stratigraphically complex Kingston Peak Formation (Miller, 1985; Prave, 1999a), which contains two distinct diamictites separated variably by siltstone, sandstone, conglomerate, and two thin carbonate units (Fig. 3; Miller, 1985; Prave, 1999a; Corsetti et al., 2003). The older Surprise diamictite is highly variable in thickness (<300 m) and contains intrabasinal clasts. Locally, it is overlain by the thin, Sourdough Limestone Member (Miller, 1985), which is intercalated with the underlying Surprise diamictite and gradational into overlying shale of the South Park Member (Miller, 1985). The younger Wildrose diamictite disconformably overlies the isotopically positive "Unnamed" Limestone Member and is dominated by basement clasts (Prave, 1999a). It is capped by the extensive Noonday Dolomite, which is remarkably similar lithologically (Cloud et al., 1974) and isotopically (Prave, 1999a; Corsetti and Kaufman, 2003) to the basal cap dolostone (Keilberg Member) of the Maieberg Formation in northern Namibia (Corsetti and Kaufman 1999).

Prave (1999a) regarded the Surprise diamictite as Sturtian in age based on its location below the presumed Marinoan-aged Wildrose and the high organic content and negative $\delta^{13}C$ composition of the overlying Sourdough Limestone, which he argued to be a cap carbonate. However, Corsetti and Kaufman (2003) have documented the onset of a negative $\delta^{13}C$ anomaly in the upper Beck Spring Formation (Fig. 5), which if equivalent to the Trezona anomaly, implies that the entire Kingston Peak Formation may be Marinoan and homologous to the Polarisbreen glacials in Svalbard (Fig. 5) and their equivalents in eastern Greenland. The negative $\delta^{13}C$ composition of the Sourdough Formation, if a primary seawater signal, could then be residual from the Trezona anomaly rather than evidence for the end of glaciation.

If the Kingston Peak Formation is Marinoan, then the lower Beck Spring Formation most likely represents the Sturtian cap carbonate, based on its lithological and stratigraphic similarity to the Rasthof cap carbonate in Namibia (Corsetti and Kaufman, 1999). Notably, the lower Beck Spring Formation contains deepwater sediments with debris-flow breccias, organic-rich microbialites, and purported "roll-up" structures in a >100-m-thick upward-shoaling parasequence (Corsetti and Kaufman, 2003). No glacial deposits occur on the subjacent sequence boundary, but negative $\delta^{13}C$ values, followed by a rise to +5‰, are preserved in the lower 25 m of the Beck Spring Formation

in some sections (Corsetti and Kaufman, 2003; Prave, 1999a; Fig. 5).

Corsetti and Kaufman (2003) suggest that the Rainstorm Member of the Johnnie Formation, which lies well above the Marinoan-aged Noonday Dolomite, may be a cryptic cap carbonate whose associated glacial deposits are not preserved. The ~50-m-thick, laterally persistent Rainstorm Member is very isotopically depleted ($\delta^{13}C <-8‰$; Figs. 5 and 6) and contains some lithological features typical of cap carbonates, including oolites, pink limestone, and formerly aragonite crystal fans in an otherwise clastic interval (Corsetti and Kaufman, 2003). However, the Rainstorm Member does not rest atop a major sequence boundary (or glacial deposits), as would be expected of a cap carbonate, but rather occurs beneath one (Summa, 1993). Various authors have proposed that the Johnnie paleovalley developed during a glacioeustatic fall in sea level (Christie-Blick and Levy, 1989; Abolins et al., 1999), which, based on our correlations, could correspond to the Gaskiers glaciation. If correct, it appears that this glaciation was preceded by a negative $\delta^{13}C$ anomaly of even greater magnitude than the Trezona anomaly.

Scotland

The link between the Scottish Dalradian succession and the EGES platform has been considered by many authors (e.g., Hambrey, 1983; Nystuen, 1985; Brasier and Shields, 2000), most of whom correlate the Port Askaig Tillite with glacial pairs from the North Atlantic region. More recently, several authors have argued that the Port Askaig is Sturtian, based in part on the occurrence of a putative glacial unit that occurs stratigraphically above (Fig. 5; Prave, 1999b; Condon and Prave, 2000) and on low $^{87}Sr/^{86}Sr$ in carbonates (0.7067) within the Lossit Formation, below the glacial deposits (Brasier and Shields, 2000). New $^{87}Sr/^{86}Sr$ data from the Russøya Formation (Fig. 5) in Svalbard show nearly identical values (0.7068) and strengthen the correlation of the Port Askaig Tillite with the EGES glacials. However, the upper Lossit Formation also records an 8‰ decline in $\delta^{13}C$ (Brasier et al., 2000), which more closely resembles the Trezona anomaly (Fig. 5) than the pre-Sturtian $\delta^{13}C$ record (Fig. 2). Therefore, in the context of our correlation scheme, the Port Askaig glacials are interpreted as Marinoan in age. This interpretation implies that low $^{87}Sr/^{86}Sr$ values are not unique to pre-Sturtian carbonates.

The thick (<750 m) Port Askaig Tillite is overlain by the Bonahaven Formation cap carbonate, a stromatolitic dolostone with inter-

calated sand and silt (Spencer and Spencer, 1972; Fairchild, 1980, 1985) that shares limited physical resemblance to other presumed Marinoan cap carbonates (Brasier and Shields, 2000), akin to the cap carbonate to the Egan glacials in Western Australia (Grey and Corkeron, 1998). The lower Bonahaven Formation does exhibit the typical negative carbon-isotope composition, but $\delta^{13}C$ is much more variable than in typical Marinoan cap dolostones (Fig. 5; Brasier and Shields, 2000). However, like other cap dolostones, it has high Fe and Mn concentrations (Fairchild, 1980) and shows petrographic evidence for penecontemporaneous dolomitization (Spencer and Spencer, 1972; Fairchild, 1980). Furthermore, as pointed out by Brasier and Shields (2000), the Bonahaven Formation, like the Dracoisen Formation in Svalbard (Halverson et al., 2004), records a spike to highly positive $\delta^{13}C$ values in isolated carbonates in the upper part of the formation. Most likely, the uniqueness and thickness of the Bonahaven cap dolostones, when compared to more typical Marinoan cap dolostones, is a function of a readily available source of clastics in the Dalradian basin, perhaps coupled with a high subsidence rate (Prave, 1999b) or localized block rotation. The Bonahaven Dolomite is therefore a useful reminder of the role that a depositional environment can play in the character of a cap carbonate (Hoffman and Schrag, 2002).

If the Port Askaig Tillite is Marinoan, then the purportedly glaciogenic Loch na Cille Boulder Bed (Elles, 1934; Prave, 1999b) and/or equivalent glaciogenic rocks in Ireland (Condon and Prave, 2000) may represent a post-Marinoan glaciation. The Loch na Cille stratigraphically overlies the 601 ± 4 Ma (Dempster et al., 2002) Tayvallich Volcanics and is therefore constrained to be less than ca. 600 Ma. These glacial deposits appear to lack a cap carbonate (Condon and Prave, 2000), clearly distinguishing them from the Port Askaig and other Marinoan glacials discussed above.

Neither unequivocal glacial deposits nor isotopic evidence for a Sturtian cap carbonate occur beneath the Port Askaig Tillite (see Fig. 1 in Brasier and Shields, 2000), but a possible Sturtian glacial horizon does occur in the lower Appin Group, well below the Port Askaig Tillite. Treagus (1969) interpreted the Kinlochlaggen Boulder Bed as glaciogenic and placed it in the upper Lochaber Subgroup (lower Appin Group). However, the stratigraphic position of the Kinlochlaggen Boulder Bed within the Appin Group is a matter of contention (Winchester and Glover, 1988; Evans and Tanner, 1996) and therefore cannot at present be confidently ascribed to the Sturtian glaciation in eastern Laurentia.
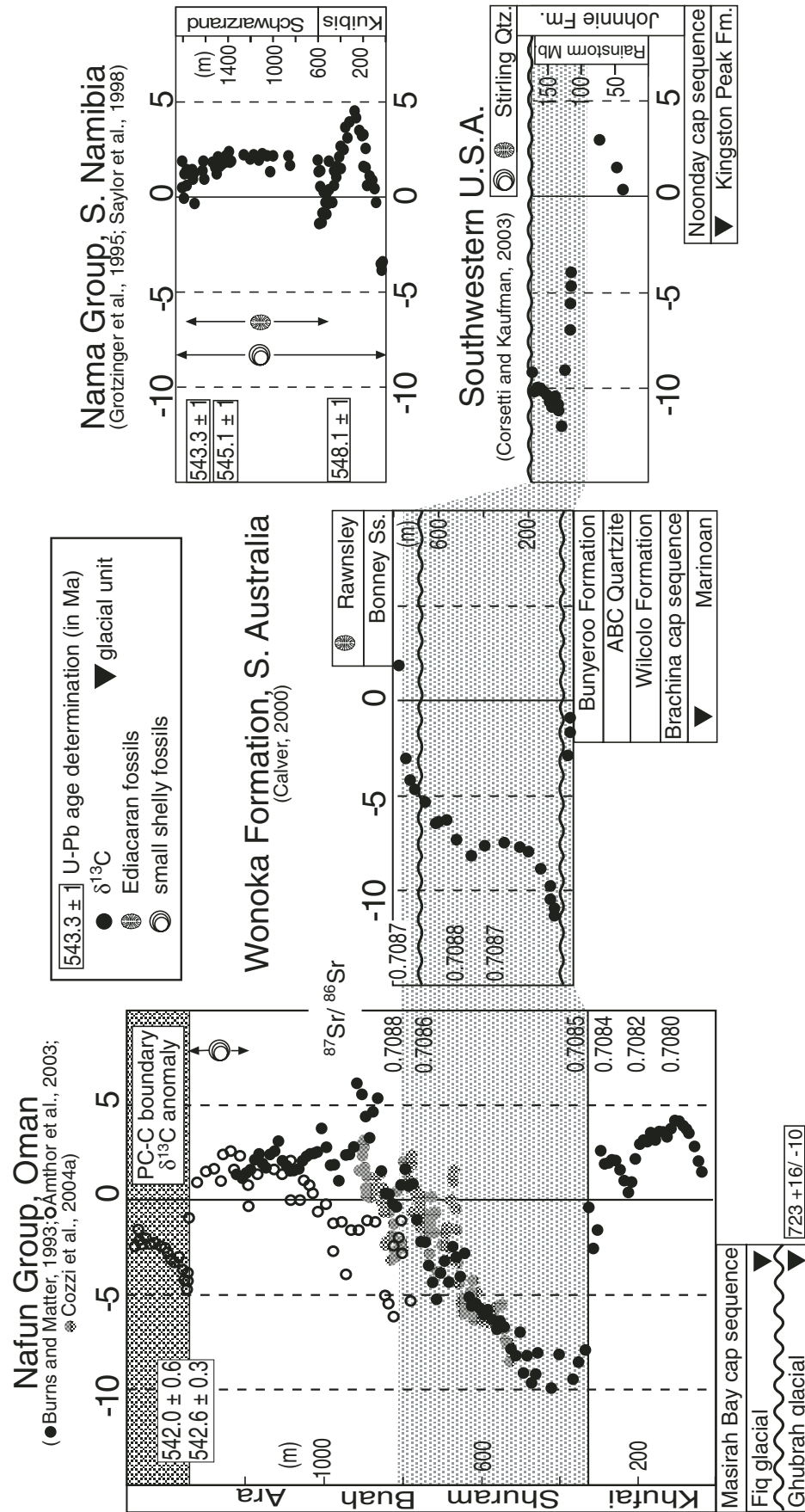
NEOPROTEROZOIC CARBON-ISOTOPE RECORD

Figure 6. Published late Neoproterozoic carbon-isotope profiles that capture the Wonoka anomaly: the Nafun Group in Oman ($^{87}Sr/^{86}Sr$ from Burns et al., 1994; U-Pb ages in Ara Group from Amthor et al., 2003 and in Ghubrah Formation from Brasier et al., 2000), the Wonoka Formation in South Australia ($^{87}Sr/^{86}Sr$ data from Calver, 2000), and the Johnnie Formation in Death Valley. The stippled pattern shows inferred correlation of the Wonoka anomaly between the three successions. Approximate position of the Wonoka paleovalleys (Christie-Blick et al., 1990) relative to the carbon-isotope profile is based on Calver (2000). The carbon-isotope profile and U-Pb ages from intercalated ash beds in the Nama Group (Grotzinger et al., 1995) indicate correlation with upper Nafun and lower Ara groups in Oman, although the Precambrian-Cambrian boundary $\delta^{13}C$ excursion (crosshatched) is missing due to erosional truncation in the former (Grotzinger et al., 1995). Recent U-Pb determinations from Oman pin the timing of the Precambrian-Cambrian boundary $\delta^{13}C$ excursion to 542 Ma and constrain the duration to <1 m.y. (Amthor et al., 2003).

Oman

Two apparently distinct Neoproterozoic glacial units occur in the Jebel Akhdar region of northern Oman (Brasier et al., 2000; Leather et al., 2002). Brasier et al. (2000) obtained a date of 723 +16/–10 Ma on a tuffaceous greywacke in the older of the two glacials, the Ghubrah Formation, and on the basis of this age interpreted it to be Sturtian. However, no cap carbonate sequence to this glacial has been identified owing to top truncation of the Ghubrah by an angular unconformity (Brasier et al., 2000). The thick (up to 1.5 km) glaciogenic Fiq Formation lies directly above the Ghubrah and consists of a series of turbidite-diamictite cycles with evidence of at least episodically open-water conditions (Leather et al., 2002). The Fiq is overlain by the Hadash cap dolostone, which forms the transgressive base of the otherwise clastic Masirah Bay cap carbonate sequence (Brasier et al., 2000). The <10-m-thick Hadash cap dolostone sharply overlies the Fiq glacials and consists of finely laminated, ^{13}C-depleted dolomite interbedded with silt (Brasier et al., 2000; Leather et al., 2002). The Hadash lacks some of the hallmark sedimentary structures of cap dolostones in other sections (e.g., megaripples and peloids), but otherwise the Masirah Bay cap carbonate sequence closely resembles other Marinoan cap carbonate sequences.

Carbonate deposition resumed at the base of the Nafun Group, above the Masirah Bay Formation (Fig. 6). The Nafun Group is well exposed both in the Jebel Akhdar and to the south along the Huqf axis (Gorin et al., 1982; Cozzi et al., 2004a, 2004b) and records the most impressive negative anomaly in the entire Neoproterozoic. δ^{13}C drops to less than –10‰ and highly negative values (<–5‰) persist through several hundred meters of section (Fig. 6; Burns and Matter, 1993). The anomaly spans the Shuram Formation, which comprises predominantly red siltstones and cross-bedded limestone grainstones (Gorin et al., 1982; Wright et al., 1990; Cozzi et al., 2004a). No significant sequence boundaries have been reported from within Shuram Formation (Wright et al., 1990), although the contact between the Shuram Formation and the underlying Khufai Formation (Fig. 6) is interpreted by Gorin et al. (1982) to represent a hardground and break in deposition. The contact between the Shuram Formation and the overlying Buah Formation is unequivocally transitional (Cozzi et al., 2004b).

δ^{13}C returns to positive values in the Buah Formation (Burns and Matter, 1993; Cozzi et al., 2004a) and remains >0‰ up to a Precambrian-Cambrian boundary anomaly in the lower Ara Group (Fig. 6; Amthor et al., 2003). Amthor et al. (2003) have constrained the duration of this large (>10‰) anomaly, which is well known globally (Magaritz et al., 1991; Knoll et al., 1995; Kaufman et al., 1996), to less than 1 m.y. and dated the Precambrian-Cambrian boundary and the abrupt disappearance of the lightly calcified fossils *Cloudina* and *Namacalathus* at 542 Ma. The combination of precise radiometric ages and detailed carbon-isotope data from the Terminal Proterozoic succession of Oman make it a useful component in the Neoproterozoic composite carbon-isotope record.

NEW DATA

Here we report new carbon-isotope data from northern Norway, Namibia, and Svalbard that contribute to the correlations and the composite carbon-isotope record. The Norway data support radiometric data indicating that there was a third, post-Marinoan (Varanger) glaciation (Knoll et al., 2004) and strengthen the connection between this event and the extraordinary negative δ^{13}C anomaly seen in Oman, Death Valley, and South Australia. New carbon-isotope data from the Tsumeb Subgroup in Namibia fill in the record between the Marinoan and Gaskiers glaciations, and a detailed data set from the Akademikerbreen Group in Svalbard establishes a long, pre-Sturtian δ^{13}C record. A radiometric age from an ash bed in the Ombombo Subgroup (pre-Sturtian) presents a new tie point for the composite record.

Northern Norway

In northern Norway, two glacial units, the Smalfjord (lower) and Mortensnes (upper) formations, with the intervening Nyborg Formation, form the base of the Vestertana Group (Fig. 5; Reading and Walker, 1966; Bjørlykke, 1967; Edwards 1975, 1984; Føyn and Siedlecki, 1980) and have commonly been correlated with the diamictite pairs on the EGES platform and elsewhere in the North Atlantic region (e.g., Hambrey 1983; Nystuen, 1985; Fairchild and Hambrey, 1995).

In the Varangerfjord area the Smalfjord Formation comprises marine and nonmarine sandstone locally interspersed with diamictites (Edwards, 1975, 1984; Arnaud and Eyles, 2002). In the nearby Tanafjord/Smalfjord area, it consists of <135 m of a heterogeneous mixture of sandstones, mudstones, conglomerates, and diamictites, recording up to five glacial advance-and-retreat cycles (Reading and Walker, 1966; Edwards, 1984). To the west, the Smalfjord Formation reaches its maximum thickness (~420 m) and comprises three separate diamictite intervals (the lower, middle, and upper Krokvatn diamictites) that infill a 350-m-deep paleovalley (Fig. 5; Føyn and Siedlecki, 1980). Analogous to the Polarisbreen Group, the upper diamictite is the thickest (<100 m) and reflects multiple glacial advance-and-retreat cycles (Edwards, 1984). The upper and middle diamictites are separated by an ~200-m-thick, monotonous sandstone, notable for the virtual absence of sedimentary structures and reminiscent of the MacDonaldryggen Formation in Svalbard.

The Smalfjord Formation is sharply overlain by the Nyborg cap carbonate sequence, whose stratigraphic, sedimentological, and isotopic characteristics clearly define it as Marinoan in age (Edwards, 1984; Rice et al., 2001). δ^{13}C consistently ranges from –2‰ to –4‰ (Fig. 5) and barite crystal fans up to 2.5 cm tall occur in one locality. The Nyborg cap dolostone is commonly overlain by an interval of red shales and siltstones with thin dolostone intercalations (Edwards, 1984), which then pass upward into 350 m of turbiditic sandstones and shales deposited during a sea-level highstand (Edwards, 1984).

The ~260-m-thick Grasdal Formation (Tanafjord Group), which occurs beneath the Smalfjord Formation in the Trollfjord area, is an isolated carbonate sequence within an otherwise siliciclastic succession (Siedlecka and Siedlecki, 1971). It comprises thin dolomites and marls at the base, passing up into massive gray stromatolitic dolomites, then alternating dolomites and argillites at the top of the formation. The Grasdal and Smalfjord formations are separated by a 20-m-thick unit of black shale and sandstone (Føyn and Siedlecki, 1980). Within the upper Grasdal Formation, δ^{13}C drops from a high of +6‰ down to –2‰ over 120 m of section, before rising again to +3‰ (Fig. 5). Considering the negative δ^{13}C anomalies both above and below the Smalfjord Formation and the characteristics of the Nyborg Formation cap carbonate sequence, it is inescapable to conclude that the Smalfjord Formation represents only the Marinoan glaciation and thus correlates with both Polarisbreen diamictites in Svalbard and not just the older, Petrovbreen diamictite. This correlation is supported by the development of a thick, multiple diamictite sequence in the Krokvatn area (Føyn and Siedlecki, 1980), comparable to the Polarisbreen glacial sequence (Halverson et al., 2004).

The Mortensnes Formation, which locally cuts down through the ~400-m-thick Nyborg Formation and into the Smalfjord Formation, is much thinner (<50 m) than the Smalfjord Formation but contains striated clasts and lonestones and is generally accepted as glacial in origin (Edwards, 1984). Its presence above the

Marinoan-aged Smalfjord diamictite is consistent with the occurrence of a third Neoproterozoic glaciation. However, unlike the Marinoan and Sturtian glacial deposits, the Mortensnes Formation lacks a cap carbonate and is instead overlain by fluviatile and deltaic sandstones and shales of the Stappogiedde Formation (Edwards, 1984). This is a key distinction since it presents the possibility that this glaciation was diachronous and not a snowball event. Nonetheless, the Mortensnes Formation is also associated with a large, albeit sparsely documented, negative $\delta^{13}C$ anomaly, with $\delta^{13}C$ values as low as –8‰ (Fig. 5) preserved in a 2-m-thick dolomite bed ~10 m below the Mortensnes Formation (Edwards, 1984). Taking into consideration that values this low do not occur in any other cap carbonate sequence and that the lowest values in the Maieberg Formation (Fig. 2) occur just above the cap dolostone (Hoffman et al., 1998a), then it seems that the very low $\delta^{13}C$ values in the upper Nyborg Formation (Fig. 5) must represent a portion of a distinct, post-Marinoan anomaly.

Age constraints on the Neoproterozoic succession in Finnmark are few since no robust isotopic ages have been obtained from the Vestertana and Tanafjord Groups. The oldest Ediacaran fauna in the succession, which consist of simple disks interpreted by Gehling et al. (2000) as synonyms of *Aspidella,* occur in the Innerelv Member of the Stappogiede Formation, ~200 m above the Mortensnes Formation (Farmer et al., 1992). The lowermost Ediacaran fossils in the Conception Group (Avalon Peninsula, Newfoundland) are younger than 575 Ma and, analogous to those in northern Norway, occur not far above the glacial diamictites of the Gaskiers Formation (Narbonne and Gehling, 2003). If the Mortensnes Formation is equivalent to the Gaskiers, which is plausible given their similar stratigraphic position relative to the lowest occurrence of Ediacaran fossils, then it records a short-lived glaciation at 580 Ma (Bowring et al., 2003).

Northern Namibia

Ombombo-Ugab Subgroups

The Ombombo Subgroup comprises mixed shallow marine carbonates and siliciclastics (Fig. 7). On the northern platform the Ombombo exceeds 700 m in thickness, but uplift of the basement high resulted in progressive southward beveling beneath the Chuos Formation (Fig. 3). An ~10-cm-thick ash bed in the middle Ombombo Subgroup on the northern platform (Figs. 3 and 7) was originally dated by the U-Pb zircon method at 758 ± 4 Ma and cited in Hoffman et al. (1998b). Here we present a more

precise age on the same sample. The sample contains a population of clear, prismatic zircons that range in size and morphology from slender 100 × 20 micron grains to more equant 50 × 40 micron grains. Eight single zircon grains were analyzed according to laboratory procedures discussed in Table DR-7 (see footnote 1) and Schmitz et al. (2003). The data define a linear array on a concordia diagram (Fig. 8B), regression of which yields an upper intercept of 759.3 ± 1.3 Ma (MSWD = 0.37). This date is indistinguishable from the weighted mean $^{207}Pb/^{206}Pb$ date (Fig. 8B) of 759.95 ± 0.86 (MSWD = 0.53), which we consider the best estimate for the age of these zircons and, inferentially, the age of the ash bed.

This age is significantly older than the 746 ± 2 Ma Naauwpoort Volcanics and slightly older than the 756 ± 2 age on the Ois Syenite (Hoffman et al., 1996), which provides a maximum age on sedimentation on the southern margin of the Congo craton. These ages imply that most if not all of the Ombombo Subgroup is older than the Ugab Subgroup, which underlies the Chuos glacials on the southern margin (Fig. 3). We tentatively correlate the upper Ombombo Subgroup (Okakuyu Formation), which contains a basalt-clast conglomerate, with the Naauwpoort Volcanics (Figs. 3 and 7) to the south. This correlation implies that the more than 700 m of mixed carbonates and clastics of the Ugab Subgroup fill in a portion of the sedimentary record missing on the northern platform, thereby providing a more complete $\delta^{13}C$ record leading into the Sturtian-aged Chuos glaciation.

$\delta^{13}C$ through the Ombombo and most of the Ugab is >0‰, but lighter values clustering around 0‰ occur in the uppermost Ugab (Fig. 7). These data suggest that a trend toward less ^{13}C-enriched carbonates presages the Sturtian glaciation, but it appears distinct from the Trezona anomaly in that it does not define a smooth and continuous decline to values as low as –5‰. Nor have heavily ^{13}C-depleted carbonates been found immediately beneath Sturtian glacial deposits in other successions (Fig. 2). Therefore, we tentatively assume that no large, preglacial negative $\delta^{13}C$ anomaly preceded the Sturtian glaciation, although more work is clearly needed to elucidate the still poorly documented $\delta^{13}C$ record leading into the Sturtian glaciation.

Abenab Subgroup

The Abenab Subgroup features two negative $\delta^{13}C$ anomalies: one at the base, in the Rasthof cap carbonate, and another in the upper Ombaatjie Formation, beneath the Ghaub diamictite (Fig. 9; Halverson et al., 2002). These anomalies are separated by an interval of

generally highly ^{13}C-enriched carbonates (Keele Peak: $\delta^{13}C$ = +5‰ to +9‰), typical of interglacial carbonates (Fig. 2; Kaufman et al., 1997). Figure 9 presents new data spanning the Abenab Subgroup from three paleogeographic regions on the Otavi platform: outer, middle, and inner shelf (Fig. 3). These data are not significantly different from previously published data through this interval (Hoffman et al., 1998a; Halverson et al., 2002), but plotted together, reveal two important features of the Namibian carbon-isotope record. First, the major trends are highly reproducible along a transect of the continental shelf. Second, the $\delta^{13}C$ compositions vary along the transect, with inner shelf sections generally enriched by 1‰–2‰ compared to middle and outer shelf carbonates. We infer that the outer shelf carbonates most faithfully record seawater $\delta^{13}C$, as presumably they were deposited closer to the open ocean south of the Congo craton (Halverson et al., 2002). We interpret these paleogeographic isotope gradients as a manifestation of regional hydrological effects (i.e., increased restriction landward) and regard the variation as a measure of the intrinsic isotopic scatter to be expected in Neoproterozoic $\delta^{13}C$ records derived from platform carbonates.

Tsumeb Subgroup

The carbon-isotope profile of the 300–400-m-thick Marinoan-aged Maieberg Formation cap carbonate sequence has been published previously (Kennedy et al., 1998; Hoffman et al., 1998a; Hoffman and Schrag, 2002), and Kaufman et al. (1991) published a reconnaissance record of the entire Tsumeb Subgroup. This previous work is supplemented here with detailed isotopic profiles through >1400 m of platform carbonates from multiple sections on the Otavi platform and a complementary 450 m profile through the Karibib Formation, the condensed foreslope equivalent (Outjo basin) of the Tsumeb Subgroup (Figs. 3 and 10). Since most post-Marinoan successions are predominantly siliciclastic, the Tsumeb Subgroup is a key element in the reconstruction of the late Neoproterozoic $\delta^{13}C$ record.

The prominent features in the Tsumeb isotope profile are (1) the smoothly varying and generally low $\delta^{13}C$ through the Maieberg and Elandshoek formations, (2) a sharp spike toward very high $\delta^{13}C$ at the top of the Elandshoek Formation, and (3) extreme variability in $\delta^{13}C$ throughout the Hüttenberg Formation. The erratic $\delta^{13}C$ pattern in the upper Tsumeb Group, including several samples that are <0‰, is a common feature of all Hüttenberg sections, but is suspicious since it is not reproduced in the foreslope section. Secondary alteration is the most obvious culprit, but the magnitude of
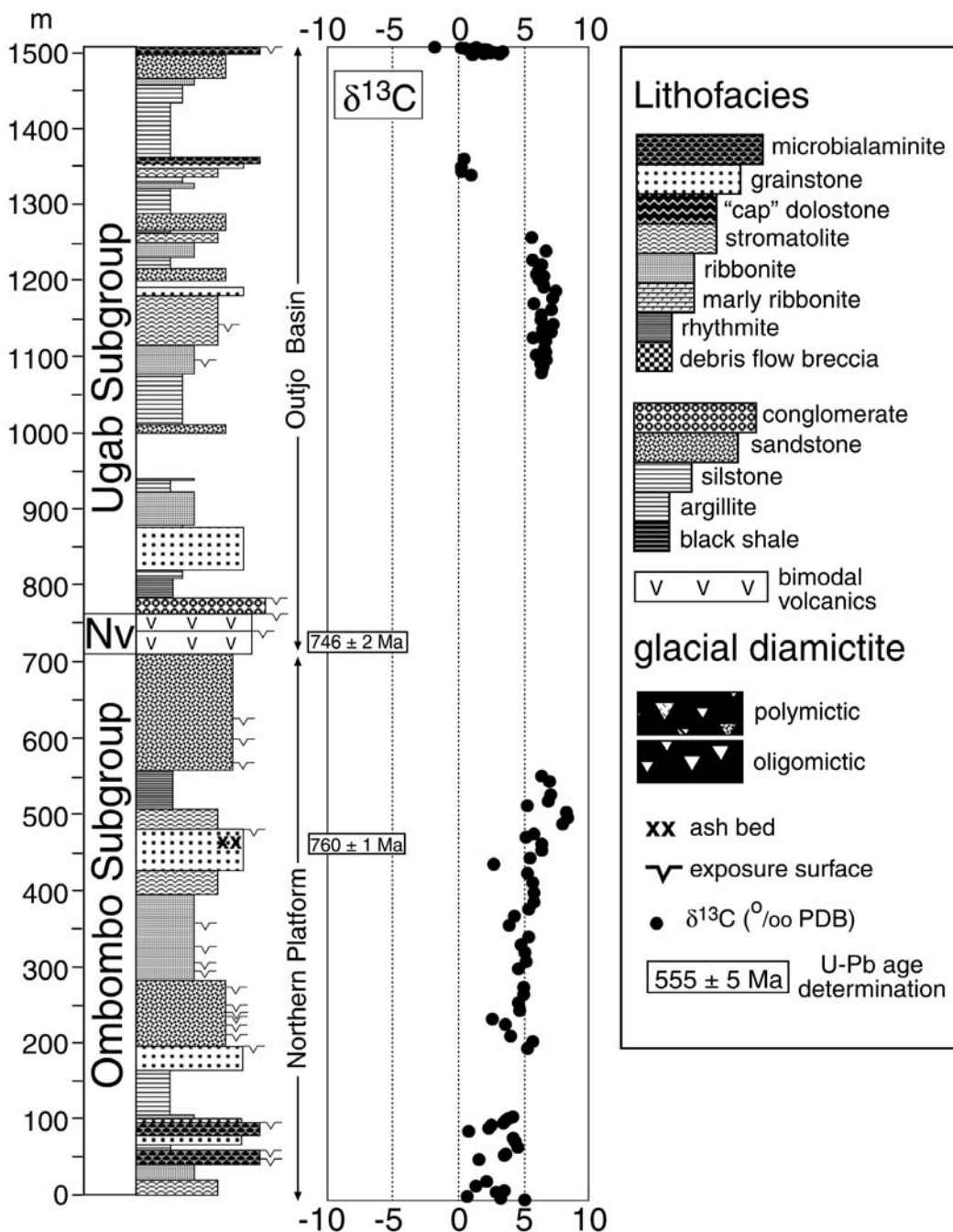
Figure 7. Composite stratigraphic section and carbon-isotope profiles (Tables DR-1; see footnote 1) of the Ombombo-Ugab Subgroups. The Ombombo Subgroup occurs exclusively on the Otavi platform, north of the Makalani rim (Fig. 3). The Ugab Subgroup occurs to the south of the Huab rim (Outjo basin) and based on U-Pb age constraints (Fig. 3) is younger than the Ombombo Subgroup. We correlate a basalt-clast conglomerate in the the upper Ombombo Subgroup (Okakuyu Formation) with the Naauwpoort Formation (which Hoffmann et al., 2004 include in the upper Nosib Group in the Outjo basin), implying that the Ugab Subgroup carbon-isotope profile fills in a record entirely missing on the Otavi platform.

variation seems large when compared to the much narrower range in alteration typical of the Otavi Group (Halverson et al., 2002). If the pattern is primary, it could have been amplified by a reservoir effect, in which restriction could be attributed to either Pan African closure of the adjacent Damaran and Brazilide seaways (Stanistreet et al., 1991) or large eustatic drops in sea level. Alternatively, the variability could be a primary seawater signal whose apparent irregularity is enhanced by a low sedimentation rate.

This hypothesis is consistent with our subsidence modeling (Halverson et al., 2002), which indicates that the upper Tsumeb Subgroup was deposited in the waning stage of a passive margin when production of accommodations space would have been slow, but cannot account for the absence of variability in the equivalent foreslope strata. A robust interpretation of the lower Hüttenberg isotope pattern will require additional, detailed data and comparison with synchronous records elsewhere.

The general $\delta^{13}C$ pattern through the Tsumeb Subgroup is captured in the equivalent Karibib Formation on the foreslope of the Outjo basin (Figs. 3 and 10). Peaks in $\delta^{13}C$ near the top and bottom of the Elandshoek Formation, as well as a nadir in the middle Elandshoek, are reproduced in the Karibib Formation, albeit with absolute values varying by a few per mil (Fig. 10). Data in the middle part of foreslope record are more scattered than data from the inferred equivalent level on the platform (Fig. 10), but this irregularity is
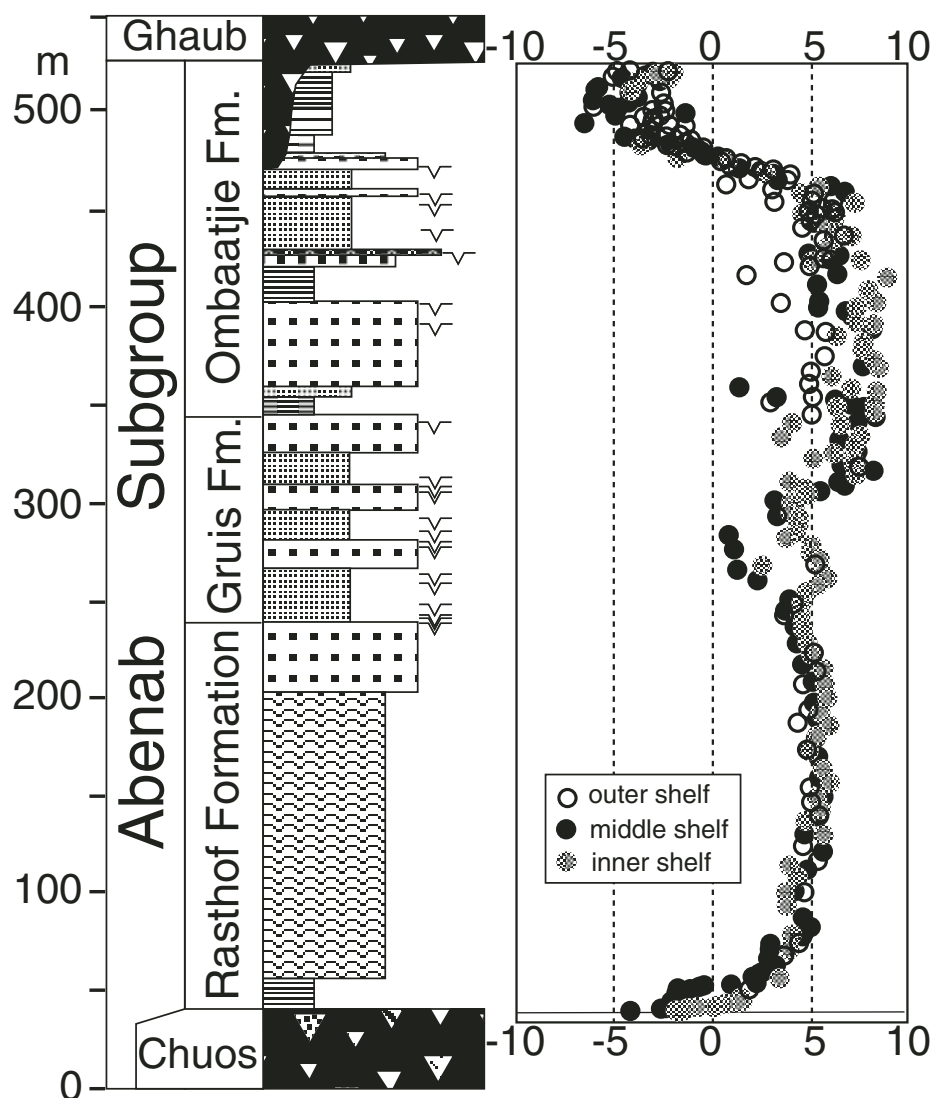
Figure 8. (A) U-Pb Concordia diagram based on six zircons from sample PH.16A.93 from an ash bed in the Ombombo Subgroup (Fig. 7). Error ellipses are plotted at the 2σ level. (B) Inset shows $^{207}Pb/^{206}Pb$ ages, the average of which (760 ± 0.9 Ma) is assumed to be the age of the ash bed. See Table DR-7 (see footnote 1) for data and explanation of procedures.

1997). Since no more than one negative $\delta^{13}C$ anomaly has been documented between the post-Marinoan anomaly and the Precambrian-Cambrian excursion (Fig. 6), the most parsimonious inerpretation is that this downturn represents the same anomaly recorded in the Johnnie and upper Nyborg formations and is therefore associated with the Gaskiers glaciation (Fig. 5).

Northeastern Svalbard

Polarisbreen Group

Figure 11 presents a composite stratigraphic and carbon-isotope record through the Polarisbreen Group (modified from Halverson et al., 2004), along with new $^{87}Sr/^{86}Sr$ data (Table DR-6; see footnote 1) from well-preserved limestones in the Russøya Member. The least radiogenic carbonates in the lower Russøya Member have a strontium isotope ratio of 0.7068, supporting correlation of this sequence with Sturtian cap carbonates (Halverson et al., 2004). A similar value in the uppermost Russøya (Fig. 11), just below the Petrovbreen diamictite, is nearly identical to values obtained by Brasier and Shields (2000) from the Lossit Limestone in Scotland (Fig. 5). If more radiogenic data (>0.7070) typical of interglacial carbonates elsewhere (Fig. 2; Kaufman et al., 1997; Jacobsen and Kaufman, 1999) accurately record seawater $^{87}Sr/^{86}Sr$, then the new Svalbard data indicate that $^{87}Sr/^{86}Sr$ declined sharply leading into Marinoan glaciation and may provide an important constraint on models to account for the Trezona $\delta^{13}C$ anomaly.

Akademikerbreen Group

The Akademikerbreen Group comprises up to 2 km of virtually uninterrupted, stromatolite-rich, platform carbonates, subdivided into the Grusdievbreen, Svanbergfjellet, Draken, and Backlundtoppen formations and continuous below with the Veteranen Group clastics (Fig. 4; Wilson, 1958, 1961; Knoll and Swett, 1990). The Akademikerbreen carbonates are generally enriched in ^{13}C, with the highest $\delta^{13}C$ values occurring in the upper Backlundtoppen Formation (Fig. 12). A prominent exception to this trend occurs in the upper Grusdievbreen and lower Svanbergfjellet formations where –3‰ <$\delta^{13}C$ <0.5‰ through ~300 m of section. This interval is bracketed by two prominent sequence boundaries, which, along with the isotopically negative carbonates, occur along the length of the outcrop belt in northeastern Svalbard (Fig. 4). These sequence boundaries stand out in the highly conformable Akademikerbreen carbonates, within which exposure surfaces are rare (Knoll and Swett, 1990). Only minor erosional truncation of the strata beneath the lower

not surprising since the foreslope strata consist of redeposited sediments, likely derived from various stratigraphic levels on the upper slope and shelf margin. $\delta^{13}C$ remains positive up to the top of the Karibib Formation where it declines abruptly beneath the contact with the Mulden Formation. This trend is missing in the Tsumeb Subgroup, presumably due to the deep level of erosion beneath the sub-Mulden unconformity on the Otavi platform (Miller, 1997). Therefore, while redeposited foreslope sediments are not ideal for reconstructing the evolution of seawater $\delta^{13}C$, the upper Karibib Formation appears to preserve the youngest portion of the Neoproterozoic $\delta^{13}C$ record in northern Namibia.

We note that in some locations near the southern margin of the Otavi Platform, a siltstone unit (Tschudi Formation) fills a karstic disconformity atop the Karibib Formation and was deformed together with the underlying carbonates prior to deposition of the Mulden foredeep clastics (Frets, 1969; Hoffmann, 1989). This relationship indicates that the siltstone unit is genetically part of the Otavi Group and that the unconformity at the top of the Karibib Formation developed during eustatic sea-level fall and not as a result of continental collision between the Congo and Kalahari cratons, which accounts for the profound unconformity beneath the main package of Mulden foredeep sediments (Miller,

sequence boundary (G1) occurs on the outcrop scale, but locally, paleokarst penetrates at least 20 m beneath the exposure surface. Above the boundary is an ~30-m-thick, upward-shoaling parasequence, the base of which consists of green and red shale and siltstone with thin limestone intercalations that are commonly ripped up and coalesced in presumably storm-generated, coarse, intraclastic breccias. This parasequence stands out amidst a background stratigraphy consisting of pure and monotonous, mid- to proximal-shelf limestone ribbonite and intraclast breccia (Fig. 12). $\delta^{13}C$ shifts abruptly across the G1 sequence boundary from +7‰ to a low of nearly –2‰ that coincides with ~1-m-thick horizon of silty micrite choked with sea-floor cements (crystal fans), presumably pseudomorphic after aragonite, that occurs at 5–10 m above the boundary.

Above this parasequence, $\delta^{13}C$ rises to a high of ~0.5‰ near the top of the Grusdievbreen Formation, before declining erratically though grainstones and peritidal microbialite to a low of ~–3‰ below the second major sequence boundary (S1) in the lower Svanbergfjellet Formation (Fig. 12). This boundary lacks obvious erosional relief but is heavily silicified and brecciated in all sections. It is overlain by black shales that grade upward through hummocky cross-stratified marls and into a regionally persistent 3–10-m-thick *Minjaria* biostrome (Knoll and Swett, 1990). $\delta^{13}C$ is already positive in the marls and continues to rise through the *Minjaria* bed and 200 m of overlying marly and fetid rhythmites and ribbonites (Fig. 12).

Smaller-scale variations (2–5‰) in $\delta^{13}C$ are common in the Akademikerbreen Group. For example, in the middle Grusdievbreen, a transient decline to 1.5‰ occurs in a silty interval with interbeds of coarse limestone breccias similar to those above the G1 sequence boundary (Fig. 12). Fluctuations of similar magnitude occur in the upper Draken and middle Backlundtoppen formations, but these do not correspond to any notable changes in sedimentation. Nor do minor exposure surfaces at the base of and within the Draken Formation correlate with any abrupt changes in $\delta^{13}C$. Carbonates remain heavily ^{13}C-enriched into the upper Backlundtoppen Formation (Kinnvikka Member) where multiple shaley parasequences, sharp flooding surfaces, and pinnacle reefs (Fig. 12) mark the demise of the Akademikerbreen carbonate platform (Halverson et al., 2004).

New Sr-isotope data from high-Sr and low-Mn limestones in the upper Grusdievbreen and lower Svanbergfjellet formations show that $^{87}Sr/^{86}Sr$ remained low and stable at ~0.7063 across the interval of low $\delta^{13}C$, with the possible exception of a transient rise just above the
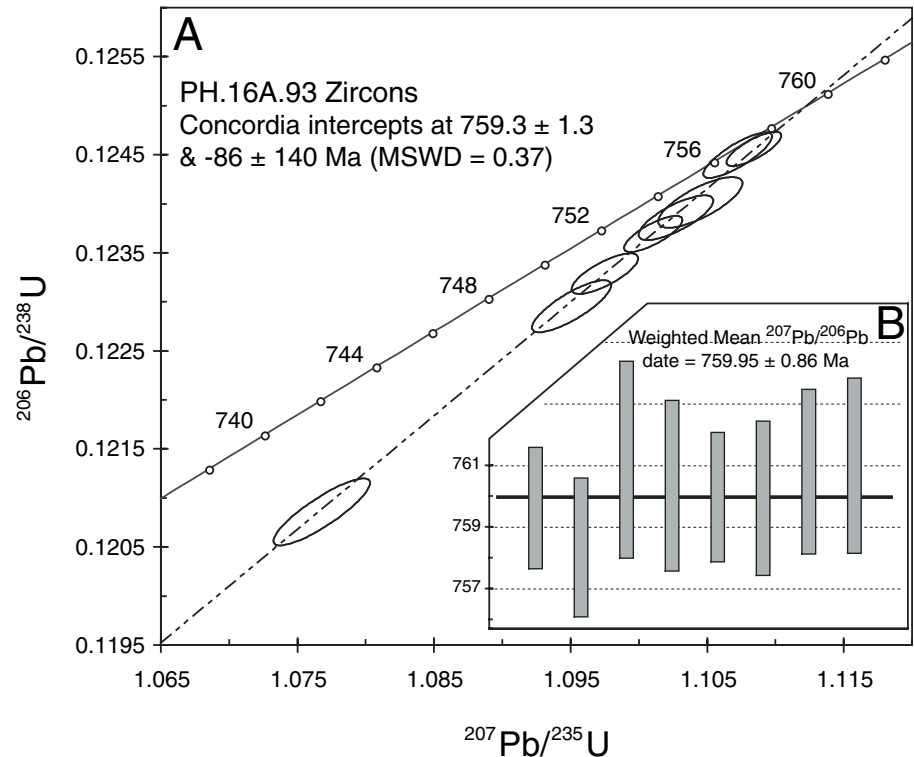

Figure 9. Composite section of the Abenab Subgroup (modified from Hoffman and Schrag, 2002 and Halverson et al., 2002). Carbon-isotope data (Table DR-2; see footnote 1) from three paleogeographic regions on the Otavi platform (Fig. 3) illustrate that while the absolute $\delta^{13}C$ values vary by 1‰–2‰ across the platform, the isotopic trends are reproducible. See Figure 7 for legend.

G1 sequence boundary (Fig. 12). These data demonstrate that the mechanism responsible for the abrupt changes in stable state of marine $\delta^{13}C$ did not significantly alter the balance between continental and hydrothermal Sr sources to seawater responsible for the relatively unradiogenic values typical of the lower Akademikerbreen Group and also provide an additional basis for correlating this interval with other successions.

DISCUSSION

The Akademikerbreen–Bitter Springs Connection

The interpretation that the lower Russøya Member in Svalbard is equivalent to Sturtian cap carbonates implies that the Akademikerbreen Group is entirely pre-Sturtian (with the possible exception of the Kinnvikka Member; Halverson et al., 2004). This hypothesis is supported by correlation of the Grusdievbreen and Svanbergfjellet formations with the Bitter Springs Formation in the Amadeus Basin, central Australia, based on their nearly identical $\delta^{13}C$ profiles (Fig. 13). The only prominent difference

between the Grusdievbreen-Svanbergfjellet and Bitter Springs profiles is a positive excursion to +5‰ within the otherwise negative $\delta^{13}C$ interval in the latter (Fig. 13). However, this spike is superimposed on a modest rise in $\delta^{13}C$ mirrored in the Svalbard section and occurs within a presumed nonmarine interval (Hill et al., 2000a; Walter et al., 2000), indicating that it may be a local signal. Sr isotope data are compatible with the correlation, but not decisive, with $^{87}Sr/^{86}Sr$ ratios generally low but highly variable in the Bitter Springs Formation (Fig. 13; Hill et al., 2000a). A test of this correlation will be whether or not ratios as low as 0.7057 can be produced in the lower Grusdievbreen Formation. Additionally, if Rainbird et al.'s (1996) lithological correlations of the Bitter Springs Formation with "Succession B" in northern Laurentia are correct, then the "Bitter Springs stage" should occur in the upper Little Dal Group (Mackenzie Mountains) and upper Shaler Supergroup (Victoria Island). Limited $\delta^{13}C$ and $^{87}Sr/^{86}Sr$ data from the Shaler Supergroup (Asmerom et al., 1991) support this correlation.

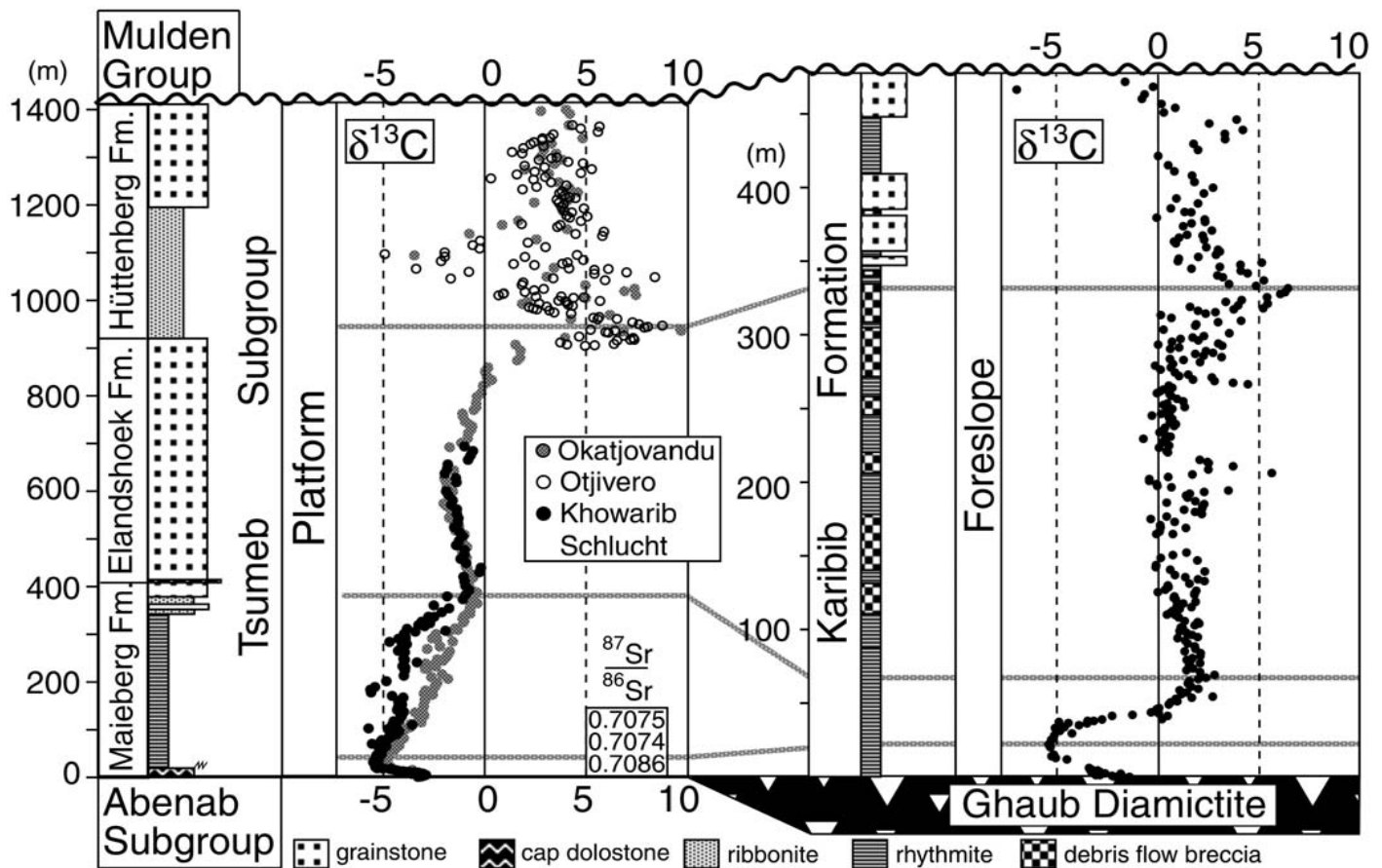The middle Akademikerbreen–Bitter Springs correlation strengthens the argument that the

Figure 10. Previously unpublished stratigraphic and carbon-isotope profiles (Table DR-3; see footnote 1) through a platform section of the Tsumeb Subgroup (left) and its foreslope equivalent, the Karibib Formation (right) in northern Namibia (Fig. 3). The Tsumeb Subgroup isotopic profile is a composite from three different sections on the inner shelf (Fig. 3). The base of the Tsumeb Subgroup is the Marinoan cap carbonate sequence (Maieberg Formation). Previously unpublished $^{87}Sr/^{86}Sr$ data in the basal Maieberg Formation (Table DR-7; see footnote 1) represent least radiogenic values. Stippled lines are approximate chronostratigraphic tie lines, based on prominent $\delta^{13}C$ data patterns reproduced in both platform and foreslope sections. If these correlations are correct, then the condensed foreslope section preserves a more complete, if less accurate, isotopic record leading up to the Mulden Group. See Figure 7 for legend.

Grusdievbreen-Svanbergfjellet $\delta^{13}C$ anomaly predates the Sturtian glaciation because the Bitter Springs Formation lies stratigraphically well below the inferred Sturtian glacial deposits (Aralka Formation) in the Amadeus Basin of central Australia (Walter et al., 1995). The Bitter Springs Formation is constrained to be younger than ca. 1000 Ma from U-Pb ages on detrital zircons in the underlying Heavitree Quartzite. Hill et al. (2000a, 2000b) argued that the upper Bitter Springs Formation is ca. 830 Ma based on strong geochemical similarity (Zhao et al., 1992) between the 827 ± 6 Ma (Wingate et al., 1998) Gairdner Dyke Swarm in the Gawler craton and volcanics interbedded within the upper Bitter Springs carbonates (Loves Creek Member). However, correlation of the Bitter Springs Formation with the isotopically light Curdimurka Subgroup (Hill et al., 2000b) in the

Adelaide geosyncline (Preiss, 2000) implies a younger age. If this correlation is correct, then the G1 and S1 sequence boundaries and the Bitter Springs isotope stage are broadly constrained to between ca. 810 and 770 Ma based on an 802 ± 10 Ma U-Pb age on the Rook Tuff (Fanning et al., 1986) in the lower Curdimurka Subgroup and the 777 ± 7 Ma Boucaut Volcanics (Preiss, 2000) in the lower Burra Group.

Three Neoproterozoic glaciations

The correlation scheme developed here supports independent evidence from recent radiometric dates (e.g., Bowring et al., 2003; Hoffmann et al., 2004) that there were three (or more) Neoproterozoic glaciations postdating ca. 750 Ma. New stratigraphic and isotopic data from northwestern China, where putative

glacial deposits from three glaciations are preserved (Xiao et al., 2004), also support this conclusion. However, despite these refinements to the Neoproterozoic chronology, significant uncertainties in the timing and global extent of the three glaciations remain. In this section we summarize the key stratigraphic, geochronological, and isotopic data that characterize each of the three glaciations.

Sturtian

Sturtian glacial deposits (Fig. 1) are best represented by diamictites in northern Namibia, South Australia, and northwestern Canada, all of which contain banded iron formation and are overlain by distinct, dark (organic- or sulfide-rich) cap carbonate sequences exhibiting a sharp, basal rise in $\delta^{13}C$ from values near –4‰ up to +5‰ (Fig. 2). Other probable Sturtian

glacials are found in southern Namibia (Fölling and Frimmel, 2002), northwestern and southern China (Evans, 2000; Hoffman and Schrag, 2002; Xiao et al., 2004), and the eastern Appalachians (Evans, 2000). Sturtian glacial deposits may also occur in Oman (Brasier et al., 2000) and Mongolia (Brasier et al., 1996). Other successions likely contain Sturtian glacials that are too poorly constrained geochronologically or stratigraphically to be assigned confidently to this age. Insofar as the correlations presented here are correct, Sturtian-aged glacial deposits are conspicuously absent in successions in the North Atlantic region (with the possible exception of Scotland), as well as the southwestern United States. Nonetheless, possible postglacial cap carbonates can be recognized in most basins based on a combination of sedimentological and isotopic characteristics. For example, in Svalbard the onset of glaciation may be manifested in the upper Akademikerbreen Group as a series of third-order cycles driven by glacioeustatic sea-level fluctuations (Halverson et al., 2004). If this hypothesis is correct, then the Sturtian ice age began with regional glaciation and did not initiate simultaneously across the globe. Glaciers, or at least sea ice, eventually could have reached the EGES platform and other pre-Iapetan basins, but without leaving much trace, analogous to the Marinoan glaciation on the Otavi platform where glacial diamictites (Ghaub Formation) are only rarely preserved (Hoffman et al., 1998a, 1998b; Halverson et al., 2002).

Donnadieu et al. (2004) proposed that the Sturtian glaciation was initiated by the rapid consumption of atmospheric CO_2 following continental break-up and enhanced silicated weathering of continental flood basalts. However, the timing of the Sturtian glaciation remains too poorly constrained to be able to link the glaciation to these events. Indeed, radiometric age determinations on the Sturtian glaciation are conflicting. The age of 746 ± 2 Ma from Naauwpoort Volcanics (Hoffman et al., 1996) in northern Namibia is the best maximum age constraint on the glaciation, but occurs over 700 m beneath the Chuos Formation (Fig. 7). This age is statistically identical to a Pb-Pb zircon evaporation date of 741 ± 6 Ma obtained by Frimmel et al. (1996) on the Rosh Pinah Volcanics in the Gariep Belt, which these authors claim interfingers with the base of the cap carbonate to the Kaigas diamictite (Frimmel et al., 2002). A similar age of 735 ± 5 Ma has been reported from volcanic pods in purported contact with the top of the Sturtian-aged Grand Conglomerate in the lower Kundelungu Group in NW Zambia (Key et al., 2001). Taken together, these three ages indicate that the Naauwpoort Volcanics, Ugab
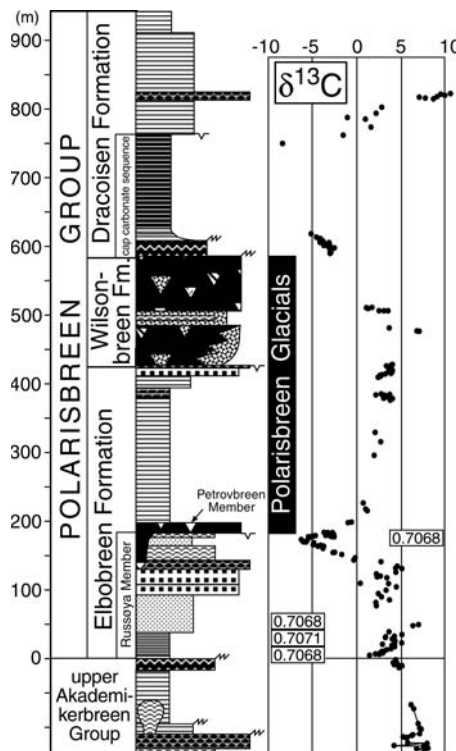

Figure 11. Stratigraphic profile and δ¹³C compilation (Table DR-5; see footnote 1) through the Polarisbreen Group (Svalbard) modified from Halverson et al. (2004). If the correlations proposed in this paper are correct, new strontium isotope data from the Russøya Member (Table DR-6; see footnote 1) indicate that ⁸⁷Sr/⁸⁷Sr was ≤0.7068 leading into the Marinoan glaciation. See Figure 7 for legend.
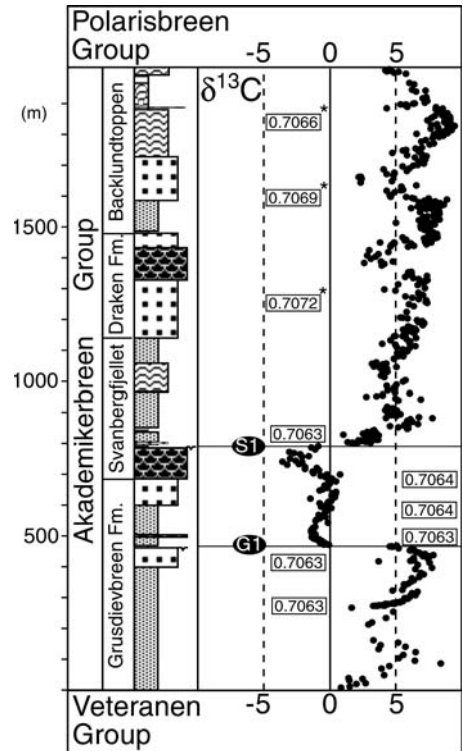

Figure 12. Simplified stratigraphic column and previously unpublished carbon-isotope compilation (Table DR-4; see footnote 1) through the Akademikerbreen Group, northeastern Svalbard (Fig. 4). G1 and S1 denote major sequence boundaries in the upper Grusdievbreen Formation and lower Svanbergfjellet Formation, respectively, which bracket a prominent interval of low δ¹³C. ⁸⁷Sr/⁸⁶Sr data from Derry et al., 1989 (*) and this paper (Table DR-6; see footnote 1). See Figure 7 for legend.

Subgroup, and Chuos Formation (Fig. 7) were all deposited in less then 13 million years. However, stratigraphic control on both the Gariep (Hoffman and Schrag, 2002) and Kundelungu ages is lacking, and we consider neither to be a robust constraint of the timing of the Sturtian glaciation.

Radiometric dates elsewhere imply a significantly younger age for the Sturtian glaciation. A U-Pb zircon age of 723 +16/–10 from an alleged ash bed within the Ghubrah diamictite in Oman (Brasier et al., 2000) is within statistical error of the above ages, but Lund et al. (2003) have obtained even younger ages of ca. 685 Ma from volcanics interbedded with what they regard as the Sturtian diamictite in metamorphosed roof pendants atop the Idaho Batholith in the northwestern United States. Similarly, Fanning and Link (2004) have constrained the timing of deposition of the purported Sturtian-aged Scout Mountain Member diamictite in southern Idaho

to between 709 ± 5 and 667 ± 5 Ma. The Idaho ages suggest that either the Sturtian glaciation is significantly younger than the commonly cited age of ca. 750–700 Ma (Fanning and Link, 2004) or that western Laurentia experienced an episode of regional glaciation between the Sturtian and Marinoan glaciations.

Marinoan

The Marinoan glaciation is presaged by a large but gradual decline in δ¹³C from highs of +5‰ to +9‰ to lows of –2‰ to –7‰, followed by a rise toward positive values in some sections. The *Trezona* anomaly has been documented in full in at least six separate successions (Figs. 2 and 5) and therefore is regarded as the record of a global event and not a regional diagenetic signal related to the Marinoan glaciation (vis-à-vis Kennedy et al., 1998). Based on a
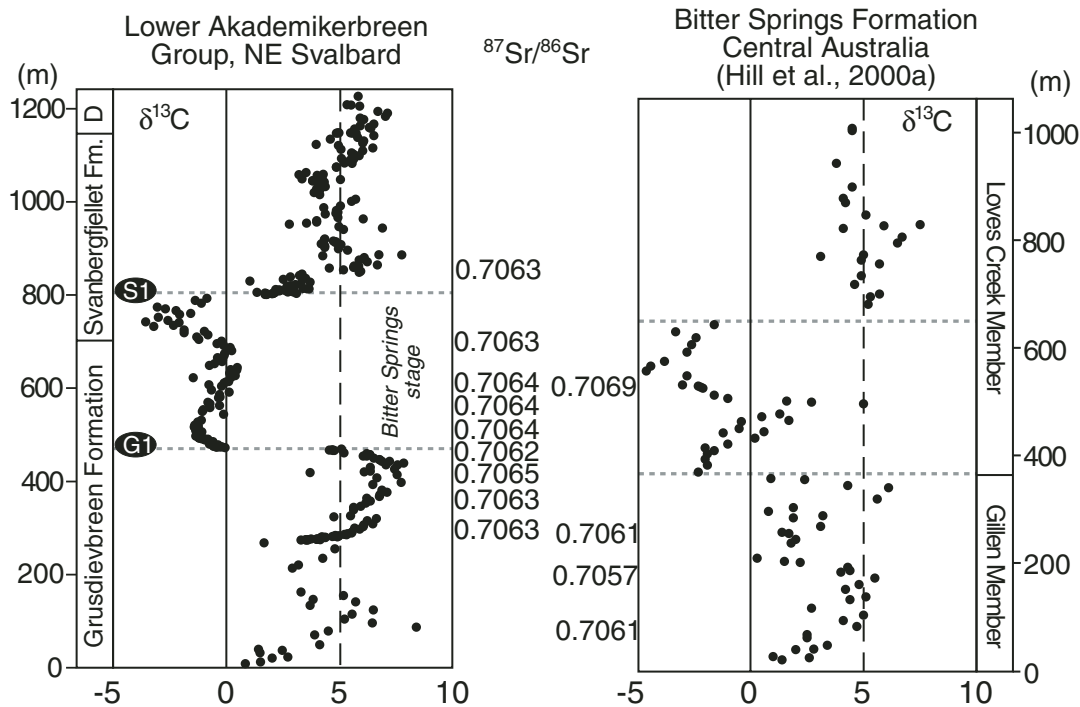
Figure 13. Isotopic profiles and $^{87}Sr/^{86}Sr$ ratios through the Grusdievbreen-Svanbergfjellet formations (Table DR-7; see footnote 1) and Bitter Springs Formation, central Australia (Hill et al., 2000a), indicating probable correlation based on chemostratigraphy. The sharp decline and rise in $\delta^{13}C$ that bracket the interval of low $\delta^{13}C$ (*Bitter Springs* stage) in Svalbard, as well as smaller sacle variations, are mirrored by the Bitter Springs profile with the exception of a positive $\delta^{13}C$ spike within the Bitter Springs stage that occurs only in Australia. However, these high $\delta^{13}C$ values are associated with a nonmarine interval (Hill et al., 2000a) and therefore may not represent contemporaneous seawater composition. Strontium isotope data support the correlation, but are not decisive, as $^{87}Sr/^{86}Sr$ in the Bitter Springs Formation is much more variable than in the lower Akademikerbreen Group in Svalbard. This correlation implies that the middle Akademikerbreen Group is entirely pre-Sturtian because the Bitter Springs Formation occurs stratigraphically well below the Sturtian glacials in central and South Australia (Walter et al., 1995; Preiss, 2000; Hill et al., 2000a).

simple thermal subsidence model for the Otavi basin in Namibia, the duration of the pre-Marinoan $\delta^{13}C$ decline is estimated to be at least 0.5×10^5 years (Halverson et al., 2002). This time scale and geological considerations preclude most commonly invoked mechanisms for driving declines in marine carbon toward mantle values (Halverson et al., 2002), and Schrag et al. (2002) proposed instead that it was caused by a protracted (but perhaps episodic) release of methane to the atmosphere from marine clathrate reservoirs.

Marinoan glacial deposits are the most widespread of the three glaciations, but are highly variable, as highlighted by the reinterpretation that the diamictites pairs on the EGES platform record the early and late stages of a Marinoan snowball cycle (Halverson et al., 2004). If this interpretation and the correlations proposed here are correct, then the Marinoan glaciation is represented by thick and complex sedimentary packages in the present-day North Atlantic region and Death Valley, in contrast to relatively simple and thin glacials in Namibia, Australia, and northwestern Canada. A Marinoan plate tectonic reconstruction is necessary to unravel the significance of systematic paleogeographic differences in the Marinoan glacial record.

Recently acquired U-Pb zircon ages indicate that the Marinoan glaciation is much older than the ca. 600 Ma age commonly cited in the literature. An ash fall tuff within the Ghaub diamictite in the Swakop zone in central Namibia (south of the Outjo basin) dated at 635.5 ± 1.2 Ma (Hoffmann et al., 2004) provides the first direct age on the Marinoan glaciation. Zhou et al. (2004) interpret the significantly older age of 663 ± 4 Ma they obtained from a tuff in the Datangpo Formation, which separates the glaciogenic Tiesiao and Nantuo formations on the southeast-facing margin of the Yangtze block in southern China, as a maximum age constraint on the Marinoan glaciation. However it is uncertain whether the glacial deposits in this sequence represent a single or multiple glacial episodes (Jiang et al., 2003a, 2003b; Zhou et al., 2004). Noting the stratigraphic similarity between the Tiesao-Datangpo-Nantuo sequence and the Polarisbreen glacial sequence in Svalbard (Fig. 11), it is tempting to speculate this tuff dates the early part of the Marinoan glaciation. The Datangpo age is statistically identical to the 667 ± 5 Ma U-Pb date from a reworked tuff in the upper Scout Mountain Member in Idaho (Fanning and Link, 2004), beneath a ^{13}C-depleted carbonate horizon resembling typical Marinoan cap carbonates. This possible Marinoan cap carbonate does not directly overlie glacial deposits and is separated from purported Sturtian-aged glacial deposits below by a pair of sequence boundaries (Lorentz et al., 2004). Therefore, analogous to the Otavi platform, Marinoan glacials may be absent from the Scout Mountain Member (Lorentz et al., 2004).

Although the Ghaub age derives from near the top of the diamictites (Hoffmann et al., 2004), an incontrovertible maximum age constraint for the end of the Marinoan glaciation will require an age from within the postglacial cap

carbonate. In the meantime, the best maximum age constraints are ca. 600 Ma (see below). This age constraint conflicts with recent U-Pb ages from a purported Marinoan glacial horizon in Tasmania, which suggests an age of ca. 580 Ma for the Marinoan glaciation in Australia (Calver et al., 2004), as well as a Re-Os age of 592 ± 14 Ma acquired from black shales beneath the Marinoan-equivalent Olympic Formation in central Australia (Schaefer and Burgess, 2003). Since the Ghaub Formation in Namibia is incontrovertibly much older, then either the stratigraphic relations in Tasmania and the Re-Os age in central Australia are incorrect or the Marinoan glacials in Australia actually correlate with the 580 Ma Gaskiers event.

Gaskiers

The glaciogenic Gaskiers Formation in eastern Newfoundland, dated at 580 Ma (Bowring et al., 2003), unquestionably represents a post-Marinoan glaciation (Knoll et al., 2004). The Gaskiers glacial deposits are almost certainly equivalent to the Squantum glacial deposits (Boston Bay Group), which outcrop further south on the Avalon terrane and are constrained to be between 570 and 595 Ma (Thompson and Bowring, 2000). An age of 601 ± 4 Ma on the Tayvallich Volcanics in Scotland (Dempster et al., 2002) is consistent with a Gaskiers age for the overlying Loch na Cille Boulder bed, which is interpreted to be glaciogenic (Prave, 1999b; Condon and Prave, 2000). This age is statistically identical to the 599 ± 4 Pb-Pb age from Duoshanto phosphorites (Barfod et al., 2002), which must have been deposited prior to the Gaskiers glaciation (Zhou et al., 2004). Along with the Quruqtagh Group in northwestern China (Xiao et al., 2004) and the Dalradian Series in Scotland, the Vestertana Group in northern Norway is a rare succession with glacial deposits (Reading and Walker, 1966; Edwards, 1984) stratigraphically above what are presumed in this paper (Fig. 1) to be Marinoan glacials. Other glacial deposits of potentially equivalent age include the Fauqier Formation in the Virginian Appalachians (Evans, 2000; Kaufman and Hebert, 2003), and, based on the distribution of acanthomorphic acritarchs (Vidal and Nystuen, 1990), the Moelv diamictite at the top of Hedmark Group in southern Norway (Knoll, 2000). Due to poor age control in most successions with presumed post-Marinoan glacial deposits and the paucity of carbonate bracketing the Gaskiers glacial deposits, it cannot yet be established that all of these glacial deposits correspond to a single glacial epoch. However, stratigraphic and carbon-isotope data reviewed below suggest that the sedimentary record of a post-Marinoan glaciation and the apparently synchronous Wonoka carbon-isotope anomaly can be identified in successions representing a wide range of paleogeographic settings.

In Norway, the Mortensnes diamictite fills a major unconformity, which may be partly attributable to glacioeustasy. A thin (<4 m) dolomite bed 20 m beneath the Mortensnes unconformity in the least truncated section (Edwards, 1984) carries a $\delta^{13}C$ signature of <–8‰ (Fig. 5) and may correlate with a shift to extremely negative values (–12‰) that occurs prior to a major sequence boundary in the upper Johnnie Formation in Death Valley (Figs. 5 and 6; Corsetti and Kaufman, 2003). Both the Johnnie Paleovalley and the Mortensnes diamictite occur above a Marinoan cap carbonate and beneath Ediacaran fossils. The correlations proposed here corroborate the hypothesis that the Johnnie paleovalley developed during a glacioeustatic lowstand (e.g., Christie-Blick and Levy, 1989). New carbon-isotope data from northwestern China also lend support to this correlation since in some sections, glacial deposits of the post-Marinoan Hankalchough Formation occur above a negative $\delta^{13}C$ anomaly (Xiao et al., 2004) of virtually identical magnitude and structure to that in Death Valley.

In South Australia the Wonoka anomaly spans a pair of major sequence boundaries (Calver, 2000), and because $\delta^{13}C$ values approximately equal to those in the upper Nyborg Formation (Fig. 5) occur beneath both surfaces (Fig. 6), it is uncertain which, if either, might correspond to glaciation. Alternatively, each Wonoka sequence boundary could correspond to glacial maxima during a single, long-lived ice age. Irrespective of this ambiguity, as no more than one extremely negative anomaly has been documented between the post-Marinoan anomaly and the Precambrian-Cambrian boundary excursion (Fig. 6), the most conservative interpretation is that the very low $\delta^{13}C$ values beneath the Mortensnes Formation and Johnnie Paleovalley (Figs. 5 and 6) record truncated segments of the Wonoka anomaly, and therefore link it temporally, if not causally, to the Gaskiers glaciation. Likewise, we conjecture that the truncated $\delta^{13}C$ anomaly in the upper Karibib Formation in Namibia represents the onset of the Wonoka anomaly. One problem with this correlation is that no major sequence boundary corresponding to the Gaskiers glaciation has been identified in Oman (Gorin et al., 1982; Cozzi et al., 2004a, 2004b). Nevertheless, insofar as the Fiq glacials are Marinoan (Brasier et al., 2000) and barring a major depositional hiatus, the Nafun Group must have spanned the Gaskiers glaciation. The absence of evidence for this glaciation in Oman does not prove that the correlations are wrong but rather emphasizes that the relationship between the Wonoka anomaly and the Gaskiers glaciation needs to be worked out.

The extremely low $\delta^{13}C$ values associated with the Wonoka anomaly and significant variability of values in inferred equivalent sections above the Hankalchoug diamictite in northwestern China (Xiao et al., 2004) make it tempting to invoke a diagenetic origin. Indeed, the anomaly is commonly preserved in organic-rich successions, and respired organic matter during burial diagenesis is certainly a plausible origin of highly ^{13}C-depleted carbon (Irwin et al., 1977). On the other hand, the anomaly is preserved through tens to hundreds of meters of section in relatively organic-lean rocks in both Death Valley and Oman, and the widespread occurrence of the anomaly suggests that local diagenesis cannot account for the global distribution of these very low values. If for now we assume that the Wonoka anomaly is a primary seawater signal, then a vast input of reactive, organic-derived carbon to the ocean (cf. Rothman et al., 2003) is seemingly required to account for the very low values. The extreme ^{13}C-depletion makes methane one candidate, but the mass that would be required to generate the full negative $\delta^{13}C$ anomaly over several hundreds of meters of section far outweighs the present reservoir of methane clathrates (between 1000 and 22,000 Gt C; Dickens, 2001). Alternatively, Rothman et al. (2003) have proposed that the transfer of ^{13}C-depleted carbon from a large reactive pool of marine-dissolved organic carbon (DOC) to the dissolved inorganic carbon pool (DIC) could explain the Neoproterozoic negative $\delta^{13}C$ anomalies. However, this model lacks a causal mechanism for glaciation and a source for the DOC, and no definitive cause can be identified for this extraordinary carbon-isotope anomaly.

The Gaskiers glacials in Newfoundland are locally overlain by a thin, ^{13}C-depleted carbonate unit, interpreted as a postglacial cap carbonate (Myrow and Kaufman, 1998). The Hankalchough diamictite in northwestern China is also overlain by carbonate, but the $\delta^{13}C$ values in this unit are highly variable (Xiao et al., 2004), unlike typical Marionan cap carbonates. The Mortensnes diamictite and the Johnnie paleovalley are both overlain by siliciclastic sediments. Therefore, unless age constraints on the glacial deposits in central Australia (Schaefer and Burgess, 2003) and Tasmania (Calver et al., 2004) prove to be correct, it appears that the Gaskiers glaciation differs from the Sturtian and Marinoan glaciations in that it was not followed by the widespread deposition of an isotopically uniform cap carbonate. The absence of a global cap carbonate to the Gaskiers glaciation would eliminate the possibility that it was a snowball event and allows that it could have been diachronous

and more typical of Phanerozoic-type ice ages (Evans, 2003). Why should this glaciation have been less severe than its predecessors? Evans (2003) has reviewed a host of possible reasons, perhaps the most significant of which are related to the paleogeographic boundary conditions to global climate. By the late Neoproterozoic the long-lived low-latitude supercontinent had dispersed and Laurentia, Baltica, southwestern Gondwana, and other continental fragments had drifted to the high latitudes (Symons and Chiasson, 1991; Torsvik et al., 1995; Evans, 2000; Meert and Torsvik, 2003). A high-latitude distribution of continents would have made it easier to nucleate continental ice sheets but would also have had global warming effects through decreased planetary albedo and weakening of the silicate weathering feedback (Schrag et al., 2002). The paleogeographic boundary conditions appear to have been sufficient to stem a snowball, despite the apparently extreme forcing evinced by the Wonoka $\delta^{13}C$ anomaly.

A Composite Carbon-Isotope Record

The correlation scheme presented here establishes the framework for a new composite $\delta^{13}C$ record for Neoproterozoic marine carbonates (Fig. 13). This $\delta^{13}C$ record should function as both a correlation tool and a metric of the biogeochemical evolution of the ocean during this eventful period in Earth history. It is analogous to the Sr-isotope curve for the Phanerozoic (Burke et al., 1982) and of particular importance for the Neoproterozoic given the limited applicability of biostratigraphy during this time period. Previous Neoproterozoic $\delta^{13}C$ compilations (e.g., Hayes et al., 1999; Jacobsen and Kaufman, 1999; Walter et al., 2000) were constructed by stitching together fragmentary records based on poorly constrained age assignments, some of which conflict with those proposed herein. The most important attribute of the composite section presented here is that it consists mostly of high-resolution data from just two successions, the Otavi Group (Namibia) and Hecla Hoek (Svalbard), which are linked through multiple tie lines (the Marinoan and Sturtian cap carbonates and the Trezona anomaly). The latest Neoproterozoic record, beginning with the Wonoka anomaly, is filled in with published data from the Nafun Group, Oman (Fig. 6), which includes the prominent and now precisely dated negative $\delta^{13}C$ excursion straddling the Precambrian-Cambrian boundary (Amthor et al., 2003). The link between the Namibian and Oman sections is based on our interpretation that the downturn in $\delta^{13}C$ in the uppermost Karibib Formation (Tsumeb Subgroup equivalent) in Namibia represents the onset of the Wonoka anomaly

(Fig. 10). However, we acknowledge that this link is the weakest in the composite record and needs to be tested.

The few pertinent U-Pb ages available from the Otavi Group and Nafun Group are shown alongside the composite $\delta^{13}C$ curve in Figure 14. A time scale is omitted in this figure because solid age constraints are few, and the Neoproterozoic chronology remains poorly time-calibrated. This said, a time scale is imperative if we are to interpret the record, compare it to other databases, and use it to date indirectly other successions that can be correlated to it. It is doubtful that the above successions will yield sufficient high-precision radiometric dates in the near future to calibrate the record internally, and the only alternative is to import radiometric ages from other successions. Inserting these ages into the composite record requires correlations based either on glaciations or $\delta^{13}C$ patterns ("wiggle matching") and other marine proxy records. Such correlations are inherently interpretative (Knoll and Walter, 1992) and are prone to invalidation as new data become available.

In Figure 15, we present two alternative calibrations based on contrasting interpretations of available U-Pb ages reviewed in the previous section. $\delta^{13}C$ data from several other successions, including those with applicable radiometric ages, are plotted, both to illustrate the lines of correlation and to portray more accurately the intrinsic scatter in the isotopic data. In the two plots, the time axes are scaled linearly between available ages. This technique is admittedly oversimplified. Once more radiometric ages become available, a more accurate method utilizing subsidence analyses will be appropriate. In the meantime, the proposed time scales should be regarded as speculative.

The composite carbon-isotope record (Figs. 14 and 15) is preliminary and will evolve as new data are produced, but even in its present state, it puts into chronological perspective the major biogeochemical events in the Neoproterozoic. Several features are worth noting. First, whereas the oceans were, on average, highly ^{13}C-enriched prior to the Marinoan glaciation, marine $\delta^{13}C$ was significantly lower afterward, despite continued high-amplitude fluctuations and at least one large positive spike in $\delta^{13}C$ (Fig. 14). This first-order shift in the steady-state $\delta^{13}C$ composition of the oceans suggests that the Marinoan glaciation had a profound and permanent effect on the Neoproterozoic environment. Among the second-order trends in the Neoproterozoic $\delta^{13}C$ record are a total of five major negative $\delta^{13}C$ anomalies/intervals. Three of these anomalies are related to the three Neoproterozoic glaciations, confirming the observed linkage between the Neoproterozoic

carbon cycle and global climate (Knoll et al., 1986). However, each of these anomalies and its temporal relationship to glaciation is distinct, implying that the mechanisms, severity, and consequences of each of the glaciations may have varied. The remaining $\delta^{13}C$ anomalies appear to be unrelated to glaciation. The first is the pronounced interval of negative $\delta^{13}C$ (Bitter Springs stage) at ca. 800 Ma that appears to be related to eustatic changes in sea level but significantly precedes the oldest known Neoproterozoic glacial deposits. The second coincides with the Precambrian-Cambrian boundary and is of similar magnitude, but appears to be short lived (<1 Ma; Amthor et al., 2003).

Many gaps and ambiguities in the record remain, including (1) the duration and timing of the Marinoan and Sturtian glaciations, (2) the duration of the Wonoka anomaly and its relationship to the Gaskiers glaciation, and (3) the duration of the pre-Sturtian record. The latter problem is particularly acute as there are no directly applicable ages older than the 760 Ma ash bed in the Ombombo Subgroup in Namibia. The dates tentatively used here are from South Australia and are tied into the record precariously through correlation with the Bitter Springs Formation (Hill and Walter, 2000; Preiss, 2000), which itself is not directly dated. Depending on the age of the Bitter Springs stage (and taking in consideration the linear interpolation of the time axis), the pre-Sturtian record shown here may extend back anywhere from 800 to 950 Ma. Even in the latter case, the early Neoproterozoic record is incomplete, but because the Bitter Springs stage appears to be a unique feature of the Neoproterozoic record, it should be possible to tack on an overlapping record to extend the composite record back in time.

CONCLUSIONS

Isotopic and stratigraphic evidence presented in this paper corroborate radiometric data that indicate that there were three Neoproterozoic ice ages between ca. 750 and 580 Ma (Knoll et al., 2004). For the sake of consistency with the recent literature, we refer to these, in order from oldest to youngest, as the Sturtian, Marinoan, and Gaskiers glaciations. A new correlation scheme is based on the consistent distinction between the cap carbonates to the Sturtian and Marinoan glaciations (Kennedy et al., 1998) and the occurrence of a distinct pre-Marinoan negative $\delta^{13}C$ anomaly (Trezona anomaly). In Svalbard, the Trezona anomaly precedes the older of a pair of diamictites (Petrovbreen) in the Polarisbreen Group, while the younger diamictite (Wilsonbreen) is overlain by a typical Marinoan-type cap carbonate sequence. From the interregional

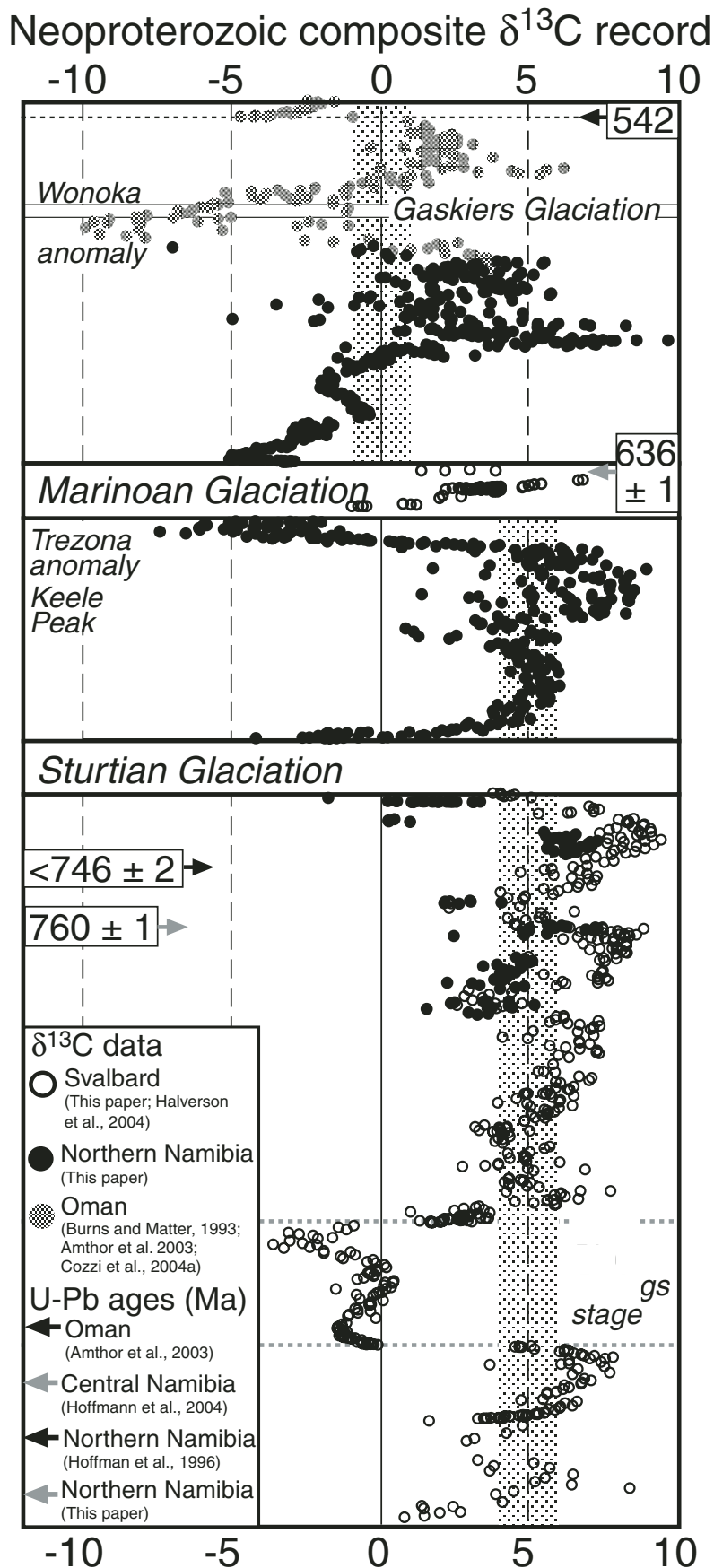## Neoproterozoic composite δ¹³C record

Figure 14. Composite carbon-isotope profile for the Neoproterozoic based on data from Svalbard, Namibia, and Oman discussed in the text. The Svalbard and Namibia records are joined based on correlation of the cap carbonate sequences to the Marinoan and Sturtian glaciations and the Trezona anomaly. The correlation between the Namibia and Oman record is less certain and based on the correlation of a downturn in δ¹³C in the uppermost foreslope section (Karibib Formation) in Namibia, interpreted as the onset of the Wonoka δ¹³C anomaly, which is well documented in Oman (Fig. 6). δ¹³C data from within the Marinoan glaciation are from the Polarisbreen Group in Svalbard and are plotted as dashed, open circles to emphasize that these may represent an isolated reservoir rather than seawater composition (Halverson et al., 2004). The relevant radiometric ages and their chemostratigraphic positions from these three successions are shown with arrows; however, due to paucity of dates, this compilation is not time-calibrated. The stippled vertical bars represent the approximate, average δ¹³C composition of the Neoproterozoic ocean prior to and following the Marinoan glaciation.
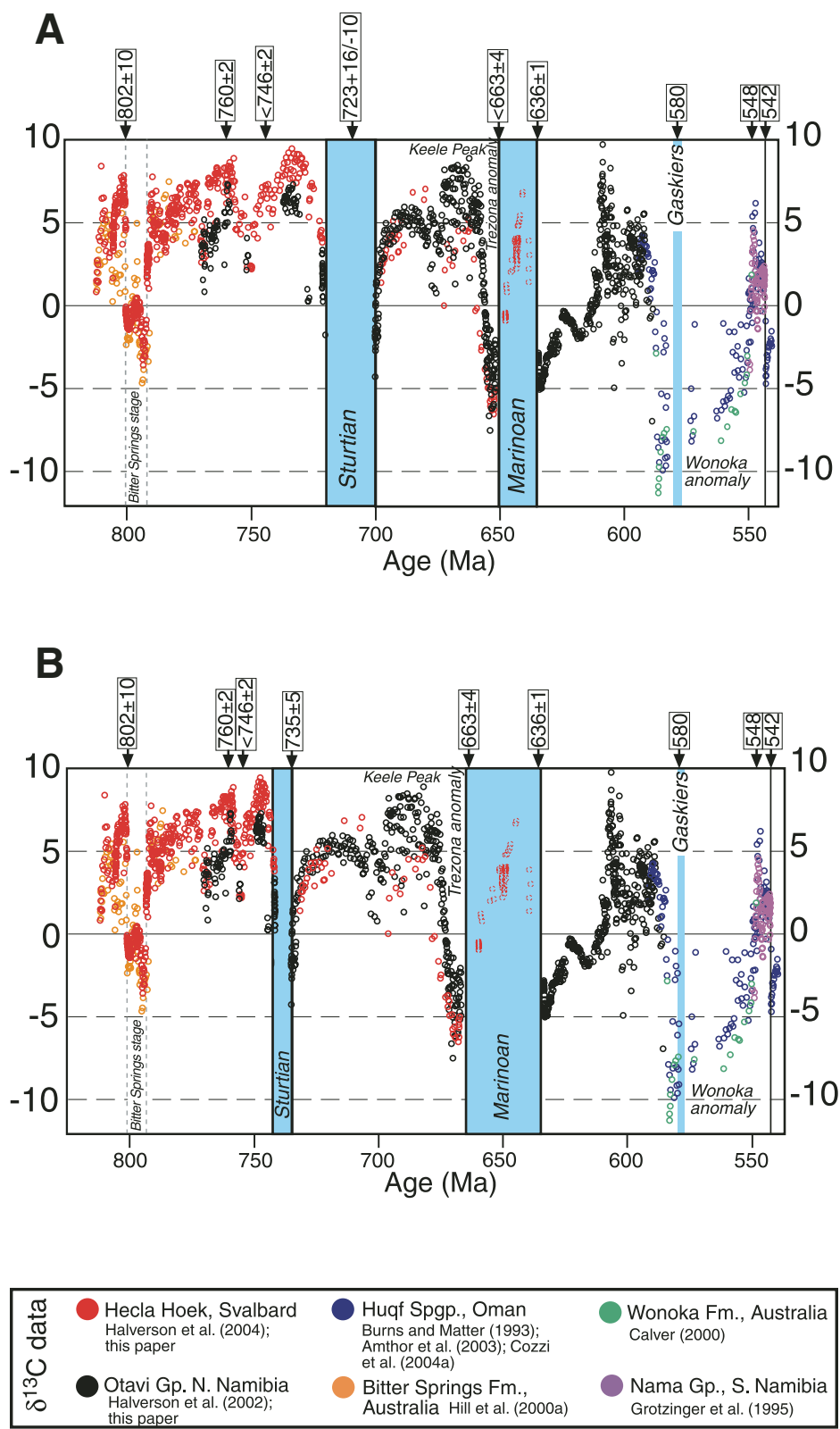
Figure 15. Two permissible calibrations of the composite carbon-isotope record in Figure 14 based on available radiometric dates and $\delta^{13}C$ data that can be correlated into the record and contrasting interpretations of the age and duration of the Sturtian and Marinoan glaciations. In both plots the following applies. (1) time is calibrated linearly between available radiometric data, (2) the base of the Bitter Springs interval is set to ca. 800 Ma based on correlations of the pre-Sturtian Neoproterozoic record between central and South Australia (Preiss, 2000) and an 802 ± 10 Ma age on the Rook Tuff in the lower Curdimurka Subgroup (Fanning et al., 1986), (3) the U-Pb age of 635.5 ± 1.2 Ma from the Ghaub Formation (Hoffmann et al., 2004) is regarded as a close approximation of the end of the Marinoan glaciation, and (4) the Gaskiers glaciation is pinned to 580 Ma based on radiometric dates from Newfoundland (Bowring et al., 2003). (A) The timing of the Sturtian glaciation is based on the assumption that minimum age constraints from the Congo (Key et al., 2001) and Kalahari (Frimmel et al., 1996) cratons are *incorrect* and that the Ghubrah diamictite in Oman is Sturtian. The 723 +16/–10 Ma age from the Ghubrah (Brasier et al., 2000) is regarded as synglacial, but neither the onset nor end of glaciation is well constrained. The timing of the onset of the Marinoan glaciation is based on the interpretation by Zhou et al. (2004) that their 663 ± 5 Ma, U-Pb age from the Datangpo Formation is a maximum age constraint on the Marinoan glaciation. (B) The Key et al. (2001) and Frimmel et al. (1996) ages alleged to date the end of the Sturtian glaciation are taken to be correct, while the maximum age constraint of 746 ± 2 Ma (Hoffman et al., 1996) requires that the Sturtian glaciation lasted less than ~10 m.y. The Datangpo age (Zhou et al., 2004) is regarded as syn-Marinoan, based on the stratigraphic similarity between the Tiesiao, Datangpo, and Nantuo Formations in southern China and the Polarisbreen glacials in Svalbard (Halverson et al., 2004). This intepretation implies that the Marinoan glaciation lasted at least 25 m.y.

perspective, it appears that the two Polarisbreen diamictites belong to the global Marinoan glaciation (Halverson et al., 2004).

Based on the same correlation criteria, the Smalfjord Formation, the older of a pair of diamictites in the Vestertana Group, northern Norway, is Marinoan in age and the younger Mortensnes diamictite is likely equivalent to the 580 Ma (Bowring et al., 2003) Gaskiers diamictite in Newfoundland. Gaskiers-aged glacial deposits are not widespread and appear to lack typical cap carbonates but are associated with a large negative $\delta^{13}C$ anomaly (Wonoka anomaly). Much work remains to be done to test the global reproducibility and stratigraphic context of this anomaly, but if it proves to be a primary seawater signal, then perhaps the most extreme deviation in marine $\delta^{13}C$ in Earth's history immediately preceded the first appearance of Ediacaran fauna.

Sturtian glacial deposits are absent or poorly represented in the North Atlantic region and the southwestern United States, but proxies for glaciation are found in the form of sequences resembling typical Sturtian cap carbonate sequences. The implied fit between the Otavi Group (Namibia) and the Hecla Hoek Succession (Svalbard) establishes a long and virtually continuous (excepting glaciations and sequence boundaries) record of the variation of marine $\delta^{13}C$ through at least half of the Neoproterozoic (Fig. 14). This record is supplemented by detailed data from Oman (Burns and Matter, 1993; Cozzi et al., 2004a; Amthor et al., 2003) that extend the record across the Wonoka anomaly to the Precambrian-Cambrian boundary (Fig. 14). Although the composite record does not yet extend backward to the base of the Neoproterozoic (1000 Ma), carbonates from the Little Dal Group and elsewhere in northern Laurentia may yet provide a deeper record.

Our model $\delta^{13}C$ record for the Neoproterozoic is incomplete and still poorly calibrated radiometrically. Its principal merit lies in its construction around only two sets of correlations between three successions with high-resolution $\delta^{13}C$ data, but these connections need to be tested. This preliminary record reproduces in detail the generally ^{13}C-enriched trends and large negative anomalies characteristic of the Neoproterozoic (Knoll et al., 1986; Hayes et al., 1999) and also highlights a salient pre-Sturtian interval of low $\delta^{13}C$ and a drop of ~5‰ in the mean carbon-isotope composition of the ocean following the Marinoan glaciation (Fig. 14). As predicted over a decade ago by Knoll and Walter (1992), this high-resolution composite $\delta^{13}C$ curve should prove a useful new tool for global correlations and the reconstruction of Neoproterozoic Earth history.

REFERENCES CITED

Abolins, M.J., Charlton, R.L., Wernicke, B.P., and Ripperdan, R.L., 1999, Three distinct glacial intervals recorded in western Laurentia and Australia: Geological Society of America Abstracts with Programs, v. 31, no. 7, p. A485.

Aitken, J.D., 1982, Precambrian of the Mackenzie fold belt—A stratigraphic overview, in Hutchinson, R.W., et al., eds., Precambrian Sulphide Deposits: Geological Association of Canada Special Paper 25, p. 149–161.

Aitken, J.D., 1989, Uppermost Proterozoic formations in central Mackenzie Mountains, Northwest Territories: Geological Survey of Canada Bulletin 368, 26 p.

Aitken, J.D., 1991a, The Ice Brook Formation and Post-Rapitan, late Proterozoic glaciation, Mackenzie Mountains, Northwest Territories: Geological Survey of Canada Bulletin 404, 43 p.

Aitken, J.D., 1991b, Two late Proterozoic glaciations, Mackenzie Mountains, northwestern Canada: Geology, v. 19, p. 445–448.

Allen, P.A., and Hoffman, P.F., 2005, Extreme winds and waves in the aftermath of a Neoproterozoic glaciation: Nature, v. 433, p. 123–127.

Amthor, J.E., Grotzinger, J.P., Schröder, S., Bowring, S.A., Ramezani, J., Martin, M.W., and Matter, A., 2003, Extinction of Cloudina and Namacalathus at the Precambrian-Cambrian boundary in Oman: Geology, v. 31, p. 431–434.

Arnaud, E., and Eyles, C.H., 2002, Glacial influence on Neoproterozoic sedimentation: The Smalfjord Formation, northern Norway: Sedimentology, v. 49, p. 765–788.

Asmerom, Y., Jacobsen, S.B., Knoll, A.H., Butterfield, N.J., and Swett, K., 1991, Strontium isotopic variations of Neoproterozoic seawater: Implications for crustal evolution: Geochimica et Cosmochimica Acta, v. 55, p. 2883–2894.

Banner, J.L., and Hanson, G.N., 1990, Calculation of simultaneous isotopic and trace element variations during water-rock interaction with applications to carbonate diagenesis: Geochimica et Cosmochimica Acta, v. 54, p. 3123–3137.

Bao, H., Xiao, S., and Yuan, X., 2004, High spatial heterogeneity of a cap-carbonate's stable-isotope signatures: A stagnant late Neoproterozoic ocean basin: Geological Society of America Abstracts with Programs, v. 36, no. 5, p. 476.

Barfod, G.H., Albarede, F., Knoll, A.H., Xiao, S., Télouk, P., Frei, R., and Baker, J., 2002, New Lu-Hf and Pb-Pb age constraints on the earliest animal fossils: Earth and Planetary Science Letters, v. 201, p. 203–212.

Bjørlykke, K., 1967, The Eocambrian "Reusch Moraine" at Bigganjargga and the geology around Varangerfjorden, northern Norway: Norges Geologiske Undersøkelse, v. 251, p. 18–44.

Bowring, S., Myrow, P., Landing, E., Ramezani, J., and Grotzinger, J., 2003, Geochronological constraints on terminal Proterozoic events and the rise of metazoans:

Geophysical Research Abstracts (EGS, Nice), v. 5, p. 13,219.

Brand, U., and Veizer, J., 1980, Chemical diagenesis of a multicomponent carbonate system—1: Trace elements: Journal of Sedimentary Petrology, v. 50, p. 1219–1236.

Brand, U., and Veizer, J., 1981, Chemical diagenesis of a multicomponent carbonate system—2: Stable isotopes: Journal of Sedimentary Petrology, v. 51, p. 987–997.

Brasier, M.D., and Shields, G., 2000, Neoproterozoic chemostratigraphy and correlation of the Port Askaig glaciation, Dalradian Supergroup of Scotland: Journal of the Geological Society of London, v. 157, p. 909–914.

Brasier, M.D., Shields, G., Kuleshov, V.N., and Zhegallo, E.A., 1996, Integrated chemo- and biostratigraphic calibration of early animal evolution: Neoproterozoic–early Cambrian of southwest Mongolia: Geological Magazine, v. 133, p. 445–485.

Brasier, M., McCarron, G., Tucker, R., Leather, J., Allen, P., and Shields, G., 2000, New U-Pb zircon dates for the Neoproterozoic Ghubrah glaciation and for the top of the Huqf Supergroup, Oman: Geology, v. 28, p. 175–178.

Burke, W.M., Denison, R.E., Hetherington, E.A., Koepnick, R.B., Nelson, M.F., and Omo, J.B., 1982, Variations of seawater $^{87}Sr/^{86}Sr$ throughout Phanerozoic time: Geology, v. 10, p. 516–519.

Burns, S.J., and Matter, A., 1993, Carbon isotopic record of the latest Proterozoic from Oman: Eclogae Geologicae Helviticae, v. 86, p. 595–607.

Burns, S.J., Haudenschild, U., and Matter, A., 1994, The strontium isotopic composition of carbonates from the late Precambrian (ca. 560–540 Ma) Huqf Group of Oman: Chemical Geology, v. 111, p. 269–282.

Calver, C.R., 2000, Isotope stratigraphy of the Ediacarian (Neoproterozoic III) of the Adelaide Rift Complex, Australia, and the overprint of water column stratification: Precambrian Research, v. 100, p. 121–150.

Calver, C.R., Black, L.P., Everard, J.L., and Seymour, D.B., 2004, U-Pb zircon age constraints on late Neoproterozoic glaciation in Tasmania: Geology, v. 32, p. 893–896.

Christie-Blick, N., and Levy, M., 1989, Stratigraphic and tectonic framework of upper Proterozoic and Cambrian rocks in the western United States, in Christie-Blick, N., et al., eds., Late Proterozoic and Cambrian Tectonics, Sedimentation, and Record of Metazoan Radiation in the Western United States: Washington, D.C., American Geophysical Union, p. 113.

Christie-Blick, N., von der Borch, C.C., and DiBona, P.A., 1990, Working hypothesis for the origin of the Wonoka Canyons (Neoproterozoic), South Australia: American Journal of Science, v. 290-A, p. 295–332.

Cloud, P., Wright, L.A., Williams, E.G., Diehl, P.E., and Walter, M.R., 1974, Giant stromatolites and associated vertical tubes from the upper Proterozoic Noonday Dolomite, Death Valley region, eastern California: Geological Society of America Bulletin, v. 85, p. 1869–1882.

Condon, D.J., and Prave, A.R., 2000, Two from Donegal: Neoproterozoic glacial episodes on the northeast margin of Laurentia: Geology, v. 28, p. 951–954.

Cordani, U.G., D'Agrella-Fiho, M.S., Brito-Neves, B.B., and Trindade, R.I.F., 2003, Tearing up Rodinia: The Neoproterozoic paleogeography of South American cratonic fragments: Terra Nova, v. 15, p. 350–359.

Corsetti, F.A., and Kaufman, A.J., 1999, Tossing Neoproterozoic snowballs between Death Valley, USA, and Namibia: A comparison of unique post-glacial facies and carbon isotope trends: Geological Society of America Abstracts with Programs, v. 31, no. 7, p. A486.

Corsetti, F.A., and Kaufman, A.J., 2003, Stratigraphic investigations of carbon isotope anomalies and Neoproterozoic ice ages in Death Valley, California: Geological Society of America Bulletin, v. 115, p. 916–932.

Corsetti, F.A., Awramik, S.M., and Pierce, D., 2003, A complex microbiota from snowball Earth times: Microfossils from the Neoproterozoic Kingston Peak Formation, Death Valley, USA: Proceedings of the National Academy of Sciences of the United States of America, v. 100, p. 4399–4404.

Cozzi, A., Allen, P.A., and Grotzinger, J.P., 2004a, Understanding carbonate ramp dynamics using $\delta^{13}C$ profiles: Examples from the Neoproterozoic Buah Formation of Oman: Terra Nova, v. 16, p. 62–67.

NEOPROTEROZOIC CARBON-ISOTOPE RECORD

Cozzi, A., Grotzinger, J.P., and Allen, P.A., 2004b, Evolution of a terminal Neoproterozoic carbonate ramp system (Buah Formation, Sultanate of Oman): Effects of basement paleotopography: Geological Society of America Bulletin, v. 116, p. 1367–1384.

Day, E.S., James, N.P., Narbonne, G.M., and Dalrymple, R.W., 2004, A sedimentary prelude to Marinoan glaciation, Cryogenian (middle Neoproterozoic) Keele Formation, Mackenzie Mountains, northwestern Canada: Precambrian Research, v. 133, p. 223–247.

Dempster, T.J., Rogers, G., Tanner, P.W.G., Bluck, B.J., Muir, R.J., Redwood, S.D., Ireland, T.R., and Paterson, B.A., 2002, Timing of deposition, orogenesis and glaciation within the Dalradian rocks of Scotland: Constraints from U-Pb zircon ages: Journal of the Geological Society of London, v. 159, p. 83–94.

Derry, L.A., Keto, L.S., Jacobsen, S.B., Knoll, A.H., and Swett, K., 1989, Sr isotopic variations in upper Proterozoic carbonates from Svalbard and East Greenland: Geochimica et Cosmochimica Acta, v. 53, p. 2331–2339.

Derry, L.A., Kaufman, A.J., and Jacobsen, S.B., 1992, Sedimentary cycling and environmental change in the lateProterozoic: Evidence from stable and radiogenic isotopes: Geochimica et Cosmochimica Acta, v. 56, p. 1317–1329.

Dickens, G.R., 2001, The potential volume of oceanic methane hydrates with variable external conditions: Organic Geochemistry, v. 32, p. 1179–1193.

Domack, E., and Hoffman, P., 2003, Stratigraphic transition into and out of a snowball glacial: Evidence from the Otavi platform and Fransfontein slope, Namibia: Eos (Transactions of the American Geophysical Union Fall Meeting, San Francisco), v. 84(46), Abstract C11B-0819.

Donnadieu, Y., Goddéris, Y., Ramstein, G., Nédélec, A., and Meert, J., 2004, A 'snowball Earth' climate triggered by continental break-up through changes in run-off: Nature, v. 428, p. 303–306.

Dunn, P.R., Thomson, B.P., and Rankama, K., 1971, Late Pre-Cambrian glaciation in Australia as a stratigraphic boundary: Nature, v. 231, p. 498–502.

Edwards, M.B., 1975, Glacial retreat sedimentation in the Smalfjord Formation, late Precambrian: North Norway: Sedimentology, v. 22, p. 75–94.

Edwards, M.B., 1984, Sedimentology of the upper Proterozoic glacial record, Vestertana Group, Finnmark, north Norway: Norges Geologiske Undersøkelse, v. 384, p. 1–76.

Eisbacher, G.H., 1978, Re-definition and subdivision of the Rapitan Group: Mackenzie Mountains: Geological Survey of Canada Paper 77-35, 21 p.

Elles, G.L., 1934, The Loch na Cille Boulder Bed and its place in the Highland Succession: Quarterly Journal of the Geological Society, v. 91, p. 111–147.

Evans, D.A.D., 2000, Stratigraphic, geochronological, and paleomagnetic constraints upon the Neoproterozoic climatic paradoxes: American Journal of Science, v. 300, p. 347–443.

Evans, D.A.D., 2003, A fundamental Precambrian-Phanerozoic shift in Earth's glacial style?: Tectonophysics, v. 375, p. 353–385.

Evans, R.H.S., and Tanner, P.W., 1996, A late Vendian age for the Kinlochlaggan Boulder Bed (Dalradian)?: Journal of the Geological Society of London, v. 153, p. 823–826.

Eyles, N., 1993, Earth's glacial record and its tectonic setting: Earth-Science Reviews, v. 35, p. 1–248.

Eyles, N., and Januszczak, N., 2004, 'Zipper-rift': A tectonic model for Neoproterozoic glaciations during the breakup of Rodinia after 750 Ma: Earth-Science Reviews, v. 65, p. 1–73.

Fairchild, I., 1980, Sedimentation and origin of a late Precambrian 'dolomite' from Scotland: Journal of Sedimentary Petrology, v. 50, p. 423–446.

Fairchild, I., 1985, Petrography and carbonate chemistry of some Dalradian dolomite metasediments: Preservation of diagenetic textures: Journal of the Geological Society of London, v. 142, p. 167–185.

Fairchild, I.J., and Hambrey, M.J., 1984, The Vendian succession of northeastern Spitsbergen: Petrogenesis of a dolomite-tillite association: Precambrian Research, v. 26, p. 111–167.

Fairchild, I.J., and Hambrey, M.J., 1995, Vendian basin evolution in East Greenland and NE Svalbard: Precambrian Research, v. 73, p. 217–233.

Fanning, C.M., and Link, P.K., 2004, U-Pb SHRIMP ages of Neoproterozoic (Sturtian) glaciogenic Pocatello Formation, southeastern Idaho: Geology, v. 32, p. 881–884.

Fanning, C.M., Ludwig, K.R., Forbes, B.G., and Preiss, W.V., 1986, Single and multiple grain U-Pb zircon analyses for the early Adelaidean Rook Tuff, Willouran Ranges, South Australia: Abstracts of the Geological Society of Australia, v. 15, p. 71–72.

Farmer, J., Vidal, G., Moczydlowska, M., Strauss, H., Ahlberg, P., and Siedlecka, A., 1992, Ediacaran fossils from the Innerelv Member (late Proterozoic) of the Tanafjorden area, northeastern Finnmark: Geological Magazine, v. 129, p. 181–195.

Fölling, P.G., and Frimmel, P.G., 2002, Chemostratigraphic correlation of carbonate successions in the Gariep and Saldania belts: Namibia and South Africa: Basin Research, v. 14, p. 69–88.

Føyn, S., and Siedlecki, S., 1980, Glacial stadials and interstadials of the late Precambrian Smalfjord Tillite on Laksefjordvidda, Finnmark, north Norway: Norges Geologiske Undersøkelse, v. 358, p. 31–45.

Frets, D.C., 1969, Geology and structure of the Huab-Welwitschia area, South West Africa: Bulletin of the Precambrian Research Unit, University of Cape Town, v. 5, 235 p.

Frimmel, H.W., Klötzli, U.S., and Siegfried, P.R., 1996, New Pb-Pb single zircon age constraints on the timing of Neoproterozoic glaciation and continental break-up in Namibia: Journal of Geology, v. 104, p. 459–469.

Frimmel, H.W., Fölling, P.G., and Erikson, P.G., 2002, Neoproterozoic tectonic and climatic evolution recorded in the Gariep Belt: Namibia and South Africa: Basin Research, v. 14, p. 55–67.

Gee, D.G., Johansson, A., Ohta, Y., Tebenkov, A.M., Krasil'schikov, A.A., Balashov, Y.A., Larinov, A.N., Gannibal, L.F., and Ryungensen, G.I., 1995, Grenvillian basement and a major unconformity within the Caledonides of Nordaustlandet: Svalbard: Precambrian Research, v. 70, p. 215–234.

Gehling, J.G., Narbonne, G.M., and Anderson, M.M., 2000, The first named Ediacaran body fossil: Aspidella Terranovica: Paleontology, v. 43, p. 427–456.

Gorin, G.E., Racz, L.G., and Walter, M.R., 1982, Late Precambrian-Cambrian sediments of Huqf Group, Sultanate of Oman: The American Associate of Petroleum Geologists Bulletin, v. 66, p. 2609–2627.

Goscombe, B., Hand, M., Gray, D., and Mawby, J., 2003, The metamorphic architecture of a transpressive orogen: The Kaoko Belt, Namibia: Journal of Petrology, v. 44, p. 679–711.

Gostin, V.A., Haines, P.W., Jenkins, R.J.F., Compston, W., and Williams, I.S., 1986, Impact ejecta horizon within late Precambrian shales, Adelaide geosyncline, South Australia: Science, v. 233, p. 198–200.

Grey, K., and Corkeron, M., 1998, Late Neoproterozoic stromatolites in glacigenic successions of the Kimberly region, Western Australia: Evidence for a younger Marinoan glaciation: Precambrian Research, v. 92, p. 65–87.

Grotzinger, J.P., Bowring, S.A., Saylor, B.Z., and Kaufman, A.J., 1995, Biostratigraphic and geochronological constraints on early animal evolution: Science, v. 270, p. 598–604.

Halverson, G.P., 2003, Towards an Integrated Stratigraphic and Carbon-Isotopic Record for the Neoproterozoic [Ph.D. thesis]: Cambridge, Massachusetts, Harvard University, 287 p.

Halverson, G.P., Hoffman, P.F., Schrag, D.P., and Kaufman, A.J., 2002, A major perturbation of the carbon cycle before the Ghaub glaciation (Neoproterozoic) in Namibia: Prelude to snowball Earth?: Geochemistry, Geophysics, Geosystems, v. 3.

Halverson, G.P., Maloof, A.C., and Hoffman, P.F., 2004, The Marinoan glaciation (Neoproterozoic) in Svalbard: Basin Research, v. 16, p. 297–324.

Hambrey, M.J., 1982, Late Precambrian diamictites of northeastern Svalbard: Geological Magazine, v. 119, p. 527–551.

Hambrey, M.J., 1983, Correlation of late Proterozoic tillites in the North Atlantic region and Europe: Geological Magazine, v. 120, p. 290–320.

Harlan, S.S., Heaman, L., LeCheminant, A.N., and Premo, W.R., 2003, Gunbarrel mafic magmatic event: A key 780 Ma time marker for Rodinia plate reconstructions: Geology, v. 31, p. 1053–1056.

Harland, W.B., Scott, R.A., Aukland, K.A., and Snape, I., 1992, The Ny Friesland Orogen, Spitsbergen: Geological Magazine, v. 129, p. 679–707.

Harland, W.B., Hambrey, M.J., and Waddams, P., 1993, Vendian Geology of Svalbard: Oslo, Norsk Polarinstitutt, Skrifter 193, 150 p.

Hayes, J.M., Strauss, H., and Kaufman, A.J., 1999, The abundance of ^{13}C in marine organic matter and isotopic fractionation in the global biogeochemical cycle of carbon during the past 800 Ma: Chemical Geology, v. 161, p. 103–126.

Hedberg, R.M., 1979, Stratigraphy of the Ovamboland Basin, South West Africa: Precambrian Research Unit Bulletin 24, University of Cape Town, 325 p.

Hegenberger, W., 1987, Gas escape structures in Precambrian peritidal carbonate rocks: Communications of the Geological Survey of Southwest Africa (Namibia), v. 3, p. 49–55.

Hill, A.C., and Walter, M.R., 2000, Mid-Neoproterozoic (ca. 830–750 Ma) isotope stratigraphy of Australia and global correlation: Precambrian Research, v. 100, p. 181–211.

Hill, A.C., Arouri, K., Gorjan, P., and Walter, M.R., 2000a, Geochemistry of marine and nonmarine environments of a Neoproterozoic cratonic carbonate/evaporite: The Bitter Springs Formation, central Australia, in Grotzinger, J.P., and James, N.P., eds., Carbonate Sedimentation and Diagenesis in an Evolving Precambrian World: Tulsa, SEPM Special Publication 67, p. 327–344.

Hill, A.C., Cotter, K.L., and Grey, K., 2000b, Mid-Neoproterozoic biostratigraphy and isotope stratigraphy in Australia: Precambrian Research, v. 100, p. 281–298.

Hoffmann, K.H., 1989, New aspects of lithostratigraphic subdivision and correlation of late Proterozoic to early Cambrian rock of the southern Damara Belt and their correlation with the central and northern Damara Belt and Gariep Belt: Communications of the Geological Survey of Namibia, v. 5, p. 59–67.

Hoffmann, K.H., and Prave, A.R., 1996, A preliminary note on a revised subdivision and regional correlation of the Otavi Group based on glaciogenic diamictites and associated cap dolostones: Communications of the Geological Society of Namibia, v. 11, p. 81–86.

Hoffman, P.F., and Schrag, D.P., 2002, The snowball Earth hypothesis: Testing the limits of global change: Terra Nova, v. 14, p. 129–155.

Hoffman, P.F., Hawkins, D.P., Isachsen, C.E., and Bowring, S.A., 1996, Precise U-Pb zircon ages for early Damaran magmatism in the Summas Mountains and Welwitschia Inlier, northern Damara belt, Namibia: Communications of the Geological Survey of Namibia, v. 11, p. 47–52.

Hoffman, P.F., Kaufman, A.J., Halverson, G.P., and Schrag, D.P., 1998a, A Neoproterozoic snowball Earth: Science, v. 281, p. 1342–1346.

Hoffman, P.F., Kaufman, A.J., and Halverson, G.P., 1998b, Comings and goings of global glaciations on a Neoproterozoic tropical platform in Namibia: GSA Today, v. 8, no. 5, p. 1–9.

Hoffman, P.F., Halverson, G.P., and Grotzinger, J.P., 2002, Are Proterozoic cap carbonates and isotope excursions the record of gas hydrate destabilization following Earth's coldest intervals?: Comment: Geology, v. 30, p. 286–287.

Hoffmann, K.H., Condon, D.J., Bowring, S.A., and Crowley, J.L., 2004, A U-Pb zircon date from the Neoproterozoic Ghaub Formation, Namibia: Constraints on Marinoan glaciation: Geology, v. 32, p. 817–820.

Ireland, T.R., Flöttmann, T., Fanning, C.M., Gibson, G.M., and Preiss, W.V., 1998, Development of the early Paleozoic Pacific margin of Gondwana from detrital-zircon ages across the Delamerian orogen: Geology, v. 26, p. 243–246.

Irwin, H., Curtis, C., and Coleman, M., 1977, Isotopic evidence for source of diagenetic carbonates formed during burial of organic-rich sediments: Nature, v. 269, p. 209–213.

Jacobsen, S.B., and Kaufman, A.J., 1999, The Sr, C, and O isotopic evolution of Neoproterozoic seawater: Chemical Geology, v. 161, p. 37–57.

James, N.P., Narbonne, G.M., and Kyser, T.K., 2001, Late Neoproterozoic cap carbonates: Mackenzie Mountains, northwestern Canada: Precipitation and global glaciation: Canadian Journal of Earth Sciences, v. 38, p. 1229–1262.

Jenkins, R.J.F., Ford, C.H., and Gehling, J.G., 1983, The Ediacara Member of the Rawnsley Quartzite: The context of the Ediacara assemblage (late Precambrian, Flinders Ranges): Journal of the Geological Society of Australia, v. 30, p. 101–119.

Jiang, G., Kennedy, M.J., and Christie-Blick, N., 2003a, Stable isotopic evidence for methane seeps in Neoproterozoic postglacial cap carbonates: Nature, v. 426, p. 822–826.

Jiang, G., Sohl, L.E., and Christie-Blick, N., 2003b, Neoproterozoic stratigraphic comparison of the Lesser Himalaya (India) and Yangtze block (south China): Paleogeographic implications: Geology, v. 31, p. 917–920.

Jefferson, C.W., and Parrish, R.R., 1989, Late Proterozoic stratigraphy, U-Pb zircon ages, and rift tectonics, Mackenzie Mountains, northwestern Canada: Canadian Journal of Earth Sciences, v. 36, p. 1784–1801.

Johansson, Å., Larianov, A.N., Tebenkov, A.M., Gee, D.G., Whitehouse, M.J., and Vestin, J., 2000, Grenvillian magmatism of western and central Nordaustlandet, northeastern Svalbard: Transactions of the Royal Society of Edinburgh, v. 90, p. 221–234.

Kaufman, A.J., and Hebert, C.L., 2003, Stratigraphic and radiometric constraints on rift-related volcanisms, terminal Neoproterozoic glaciation, and animal evolution: Geological Society of America Abstracts with Programs, v. 35, no. 6, p. 516.

Kaufman, A.J., and Knoll, A.H., 1995, Neoproterozoic variations in the C-isotopic composition of seawater: Stratigraphic and biogeochemical implications: Precambrian Research, v. 73, p. 27–49.

Kaufman, A.J., Hayes, J.M., Knoll, A.H., and Germs, G.J.B., 1991, Isotopic compositions of carbonates and organic carbon from upper Proterozoic successions in Namibia: Stratigraphic variation and the effects of diagenesis and metamorphism: Precambrian Research, v. 49, p. 301–327.

Kaufman, A.J., Knoll, A.H., Semikhatov, M.A., Grotzinger, J.P., Jacobsen, S.B., and Adams, W., 1996, Integrated chronostratigraphy of Proterozoic-Cambrian boundary beds in the western Anabar region, northern Siberia: Geological Magazine, v. 133, p. 509–533.

Kaufman, A.J., Knoll, A.H., and Narbonne, G.M., 1997, Isotopes, ice ages, and terminal Proterozoic earth history: Proceedings of the National Academy of Sciences of the United States of America, v. 94, p. 6600–6605.

Kemper, E., and Schmitz, H.H., 1981, Glendonite-Indikatoren des Polarmarinen Abagerungsmilieus: Geologische Rundschau, v. 70, p. 759–773.

Kennedy, M.J., 1996, Stratigraphy, sedimentology, and isotopic geochemistry of Australian Neoproterozoic postglacial cap dolostones: Deglaciation, δ13C excursions, and carbonate precipitation: Journal of Sedimentary Research, v. 66, p. 1050–1064.

Kennedy, M.J., Runnegar, B., Prave, A.R., Hoffman, K.H., and Arthur, M., 1998, Two or four Neoproterozoic glaciations?: Geology, v. 26, p. 1059–1063.

Key, R.M., Liyungu, A.K., Njamue, F.M., Somwe, V., Banda, J., Mosley, P.N., and Armstrong, R.A., 2001, The western arm of the Lufilian Arc in NW Zambia and its potential for copper mineralization: Journal of African Earth Sciences, v. 33, p. 503–528.

King, C.H.M., 1994, Carbonates and Mineral Deposits of the Otavi Mountain Land: Proterozoic Crustal and Metallogenic Evolution, Excursion 4: Windhoek, Geological Society and Geological Survey of Namibia Guidebook, 40 p.

Knoll, A.H., 2000, Learning to tell Neoproterozoic time: Precambrian Research, v. 100, p. 3–20.

Knoll, A.H., and Swett, K., 1987, Micropaleontology across the Precambrian-Cambrian boundary in Spitsbergen: Journal of Paleontology, v. 61, p. 898–926.

Knoll, A.H., and Swett, K., 1990, Carbonate deposition during the late Proterozoic era: An example from Spitsbergen: American Journal of Science, v. 290-A, p. 104–132.

Knoll, A.H., and Walter, M.R., 1992, Latest Proterozoic stratigraphy and Earth history: Nature, v. 356, p. 673–677.

Knoll, A.H., Hayes, J.M., Kaufman, A.J., Swett, K., and Lambert, I.B., 1986, Secular variation in carbon isotope ratios from upper Proterozoic successions of Svalbard and East Greenland: Nature, v. 321, p. 832–837.

Knoll, A.H., Kaufman, A.J., Semikhatov, M.A., Grotzinger, J.P., and Adams, W., 1995, Sizing up the sub-Tommotian unconformity in Siberia: Geology, v. 23, p. 1139–1143.

Knoll, A.H., Walter, M.R., Narbonne, G.M., and Christie-Blick, N., 2004, A new period for the geologic time scale: Science, v. 305, p. 621–622.

Leather, J., Allen, P.A., Brasier, M.D., and Cozzi, A., 2002, Neoproterozoic snowball earth under scrutiny: Evidence from the Fiq glaciation, Oman: Geology, v. 30, p. 891–894.

Lorentz, N.J., Corsetti, F.A., and Link, P.K., 2004, Seafloor precipitates and C-isotope stratigraphy from the Neoproterozoic Scout Mountain Member of the Pocatello Formation, southeast Idaho: Implications for Neoproterozoic Earth system behavior: Precambrian Research, v. 130, p. 57–70.

Lottermoser, B.G., and Ashley, P.M., 2000, Geochemistry, petrology and origin of Neoproterozoic ironstones in the eastern part of the Adelaide geosyncline, South Australia: Precambrian Research, v. 101, p. 49–67.

Lund, K., Aleinikoff, J.N., Evans, K.V., and Fanning, C.M., 2003, SHRIMP U-Pb geochronology of Neoproterozoic Windermere Supergroup, central Idaho: Implications for rifting of western Laurentia and synchroneity of Sturtian glacial deposits: Geological Society of America Bulletin, v. 115, p. 349–372.

Magaritz, M., Kirschvink, J.L., Latham, A.J., Zhuravlev, Yu, A., and Rozanov, A.Yu., 1991, Precambrian/Cambrian boundary problem: Carbon isotope correlations for Vendian and Tommotian time between Siberia and Morocco: Geology, v. 19, p. 847–850.

McKirdy, D.M., Burgess, J.M., Lemon, N.M., Yu, X., Cooper, A.M., Gostin, V.A., Jenkins, R.J.F., and Both, R.A., 2001, A chemostratigraphic overview of the late Cryogenian interglacial sequence in the Adelaide Fold-Thrust Belt, South Australia: Precambrian Research, v. 106, p. 149–186.

Meert, J.G., and Torsvik, T.H., 2003, The making and unmaking of a supercontinent: Rodinia revisited: Tectonophysics, v. 375, p. 261–288.

Melezhik, V.A., Gorokhov, I.M., Kuznetsov, A.B., and Fallick, A.E., 2001, Chemostratigraphy of Neoproterozoic carbonates: Implications for 'blind dating': Terra Nova, v. 13, p. 1–11.

Miller, J.M.G., 1985, Glacial and syntectonic sedimentation: The upper Proterozoic Kingston Peak Formation, southern Panamint Range, eastern California: Geological Society of America Bulletin, v. 96, p. 1537–1553.

Miller, R.M., 1997, The Owambo basin of northern Namibia, in Selley, R.C., ed., African Basins: New York, Elsevier Science, p. 237–268.

Myrow, P., and Kaufman, A.J., 1998, A newly discovered cap carbonate above Varanger age glacial deposits in Newfoundland, Canada: Journal of Sedimentary Research, v. 69, p. 784–793.

Narbonne, G.M., and Aitken, J.D., 1995, Neoproterozoic of the Mackenzie Mountains, northwestern Canada: Precambrian Research, v. 73, p. 101–121.

Narbonne, G.M., and Gehling, J.G., 2003, Life after snowball: The oldest complex Ediacaran fossils: Geology, v. 31, p. 27–30.

Narbonne, G.M., Kaufman, A.J., and Knoll, A.H., 1994, Integrated chemostratigraphy and biostratigraphy of the Windermere Supergroup, northwestern Canada: Implications for Neoproterozoic correlations and the early evolution of animals: Geological Society of America Bulletin, v. 106, p. 1281–1292.

Nogueira, A.C.R., Riccomini, C., Sial, A.N., Moura, C.A.V., and Fairchild, T.R., 2003, Soft-sediment deformation at the base of the Neoproterozoic Puga cap carbonate (southwestern Amazon craton, Brazil): Confirmation of rapid icehouse to greenhouse transition in snowball Earth: Geology, v. 31, p. 613–616.

Nystuen, J.P., 1985, Facies and preservation of glaciogenic sequences from the Varanger ice age in Scandinavia and other parts of the North Atlantic region: Palaeogeography, Palaeoclimatology, Palaeoecology, v. 51, p. 209–229.

Park, J.K., 1997, Paleomagnetic evidence for low-latitude glaciation during deposition of the Neoproterozoic Rapitan Group, Mackenzie Mountains, N.W.T., Canada: Canadian Journal of Earth Sciences, v. 34, p. 34–49.

Pell, S.D., McKirdy, D.M., Jansyn, J., and Jenkins, R.J.F., 1993, Ediacaran carbon isotope stratigraphy of South Australia—An initial study: Transactions of the Royal Society of South Australia, v. 117, p. 153–161.

Prave, A.R., 1999a, Two diamictites, two cap carbonates, two δ13C excursions, two rifts: The Neoproterozoic Kingston Peak Formation, Death Valley, California: Geology, v. 27, p. 339–342.

Prave, A.R., 1999b, The Neoproterozoic Dalradian Supergroup of Scotland: An alternative hypothesis: Geological Magazine, v. 136, p. 609–617.

Preiss, W.V., 2000, The Adelaide geosyncline of South Australia and its significance in Neoproterozoic continental reconstruction: Precambrian Research, v. 100, p. 21–63.

Preiss, W.V., Dyson, I.A., Reid, P.W., and Cowley, W.M., 1998, Revision of lithostratigraphic classification of the Umberatana Group: MESA Journal, v. 9, p. 36–42.

Rainbird, R.H., Jefferson, C.W., and Young, G.M., 1996, The early Neoproterozoic sedimentary Succession B of northwestern Laurentia: Correlations and paleogeographic significance: Geological Society of America Bulletin, v. 108, p. 454–470.

Reading, H.G., and Walker, R.G., 1966, Sedimentation of Eocambrian tillites and associated sediments in Finnmark, northern Norway: Palaeogeography, Palaeoclimatology, Palaeoecology, v. 2, p. 177–212.

Rice, A.H.N., Halverson, G.P., and Hofmann, C., 2001, δ13C data from Neoproterozoic cap and associated dolostones, Varanger, Finnmark, N. Norway: Proceedings, European Union of Geosciences (Strasbourg), p. A101.

Ross, G.W., and Villeneuve, M.E., 1997, U-Pb geochronology of stranger stones in Neoproterozoic diamictites, Canadian Cordillera: Implications for provenance and ages of deposition, in Radiogenic Age and Isotopic Studies, Report 10: Geological Survey of Canada Current Research 1997-F, p. 141–155.

Rothman, D.H., Hayes, J.M., and Summons, R.E., 2003, Dynamics of the Neoproterozoic carbon cycle: Proceedings of the National Academy of Sciences of the United States of America, v. 100, p. 8124–8129.

Schaefer, B.F., and Burgess, J.M., 2003, Re-Os isotopic age constraints on deposition in the Neoproterozoic Amadeus Basin: Implications for the 'Snowball Earth': Journal of the Geological Society of London, v. 160, p. 825–828.

Schmitz, M., Bowring, S.A., and Ireland, T., 2003, Evaluation of the Duluth Complex anorthositic series (AS3) zircon as a U-Pb geochronological standard: New high-precision isotope dilution thermal ionization mass spectrometry results: Geochimica et Cosmochimica Acta, v. 67, p. 3665–3672.

Schrag, D.P., Berner, R.A., Hoffman, P.F., and Halverson, G.P., 2002, On the initiation of a snowball Earth: Geochemistry, Geophysics, and Geosystems, v. 3, p. 10.1029/2001GC000219.

Shields, G., and Veizer, J., 2002, Precambrian marine carbonate isotope database: Version 1.1: Geochemistry, Geophysics, Geosystems, v. 3.

Siedlecka, A., and Siedlecki, S., 1971, Late Precambrian sedimentary rocks of the Tanafjord-Varangerfjord Peninsula, northern Norway: Norges Geologiske Undersøkelse, v. 269, p. 246–294.

Spencer, A.M., and Spencer, M.O., 1972, The late Precambrian/Lower Cambrian Bonahaven dolomite of Islay and its stromatolites: Scottish Journal of Geology, v. 8, p. 269–282.

Stanistreet, I.G., Kukla, P.A., and Henry, G., 1991, Sedimentary basinal response to a late Precambrian Wilson Cycle: The Damara Orogen and Nama Foreland, Namibia: Journal of African Earth Sciences, v. 13, p. 141–156.

Summa, C.L., 1993, Sedimentologic, Stratigraphic, and Tectonic Controls of a Mixed-Carbonate-Siliciclastic Succession: Neoproterozoic Johnnie Formation, Southeast California [Ph.D. thesis]: Cambridge, Massachusetts Institute of Technology, 616 p.

Swainson, I.P., and Hammond, R.P., 2001, Ikaite, CaCO3 • 6H2O: Cold comfort for glendonites as

paleothermometers: American Mineralogist, v. 86, p. 1530–1533.

Symons, D.T.A., and Chiasson, A.D., 1991, Paleomagnetism of the Callander Complex and the Cambrian apparent polar wander path for North America: Canadian Journal of Earth Sciences, v. 28, p. 355–363.

Thompson, M.D., and Bowring, S.A., 2000, Age of the Squantum 'tillite,' Boston basin, Massachusetts: U-Pb zircon constraints on terminal Neoproterozoic glaciation: American Journal of Science, v. 300, p. 630–655.

Torsvik, T.H., Lohman, K.C., and Sturt, B.A., 1995, Vendian glaciations and their relation to the dispersal of Rodinia: Paleomagnetic constraints: Geology, v. 23, p. 727–730.

Treagus, J.E., 1969, The Kinlochlaggan boulder bed: Proceedings of the Geological Society of London, v. 1654, p. 55–60.

Vidal, G., and Nystuen, J.P., 1990, Micropaleontology, depositional environment, and biostratigraphy of the upper Proterozoic Hedmark Group, southern Norway: American Journal of Science, v. 290-A, p. 170–211.

von der Borch, C.C., Smit, R., and Grady, A.E., 1982, Late Proterozoic submarine canyons of Adelaide geosyncline, South Australia: American Association of Petroleum Geologists, v. 66, p. 332–347.

Walter, M.R., Veevers, J.J., Calver, C.R., and Grey, L., 1995, Neoproterozoic stratigraphy of the Centralian Superbasin, Australia: Precambrian Research, v. 73, p. 173–195.

Walter, M.R., Veevers, J.J., Calver, C.R., Gorjan, P., and Hill, A.C., 2000, Dating the 840–544 Ma Neoproterozoic interval by isotopes of strontium, carbon, and sulfur in seawater, and some interpretative models: Precambrian Research, v. 100, p. 371–433.

Williams, G.E., 1979, Sedimentology, stable-isotope geochemistry and palaeoenvironment of dolostones capping late Precambrian glacial sequences in Australia: Journal of the Geological Society of Australia, v. 26, p. 377–386.

Wilson, C.B., 1958, The lower Middle Hecla Hoek rocks of Ny Friesland, Spitsbergen: Geological Magazine, v. 95, p. 305–327.

Wilson, C.B., 1961, The upper Middle Hecla Hoek rocks of Ny Friesland, Spitsbergen: Geological Magazine, v. 98, p. 89–116.

Winchester, J.A., and Glover, B.W., 1988, The Grampian Group, Scotland, in Winchester, J.A., ed., Later Proterozoic stratigraphy of the Northern Atlantic Regions: Glasgow, Blackie, p. 146–161.

Wingate, M.T.D., Campbell, I.H., Compston, W., and Gibson, G.M., 1998, Ion microprobe U-Pb ages for Neoproterozoic basaltic magmatism in south-central Australia and implications for the breakup of Rodinia: Precambrian Research, v. 87, p. 135–159.

Wright, V.P., Ries, A.C., and Munn, S.G., 1990, Intraplatformal basin-fill deposits from the Infracambrian Huqf Group, east central Oman, in Robertson, A.H.F., Searle, M.P., and Ries, A.C., eds., The Geology and Tectonics of the Oman Region: Geological Society of London Special Publication 49, p. 601–616.

Xiao, S., Bao, H., Wang, H., Kaufman, A.J., Zhou, C., Li, G., Yuan, X., and Ling, H., 2004, The Neoproterozoic Quruqtagh Group in eastern Chinese Tianshan: Evidence for a post-Marinoan glaciation: Precambrian Research, v. 130, p. 1–26.

Yeo, G.M., 1981, The late Proterozoic Rapitan glaciation in the northern Cordillera, in Campbell, F.H.A., ed., Proterozoic basins of Canada: Geological Survey of Canada Paper 810-10, p. 451–466.

Yoshioka, H., Asahara, Y., Tojo, B., and Kawakami, S., 2003, Systematic variations in C, O, and Sr isotopes and elemental concentrations in Neoproterozoic carbonates in Namibia: Implications for glacial to interglacial transition: Precambrian Research, v. 124, p. 69–85.

Young, G.M., 1995, Are Neoproterozoic glacial deposits preserved on the margins of Laurentia related to the fragmentation of two supercontinents?: Geology, v. 23, p. 153–156.

Zhao, J., McCulloch, M.T., and Bennett, V.C., 1992, Sm-Nd and U-Pb zircon isotopic constraints on the provenance of sediments from the Amadeus Basin, central Australia: Evidence for REE fractionation: Geochimica et Cosmochimica Acta, v. 56, p. 921–940.

Zhou, C., Tucker, R., Xiao, S., Peng, Z., Yuan, X., and Chen, Z., 2004, New constraints on the ages of Neoproterozoic glaciations in south China: Geology, v. 32, p. 437–440.